Late Cretaceous magmatism in the Atlin-Tagish area, northern British Columbia (104M, 104N)

A. Zagorevski[1, a], M.G. Mihalynuk[2], N. Joyce[1], and R.G. Anderson[3]

[1] Geological Survey of Canada, Ottawa, ON, K1A 0E8
[2] British Columbia Geological Survey, Ministry of Energy and Mines, Victoria, BC, V8W 9N3
[3] Geological Survey of Canada, Vancouver, BC, V6B 5J3
[a] corresponding author: alex.zagorevski@canada.ca

Recommended citation: Zagorevski, A., Mihalynuk, M.G., Joyce, N., and Anderson, R.G., 2017. Late Cretaceous magmatism in the Atlin-Tagish area, northern British Columbia (104M, 104N). In: Geological Fieldwork 2016, British Columbia Ministry of Energy and Mines, British Columbia Geological Survey Paper 2017-1, pp. 133-152.

Abstract

The Cache Creek and Stikine terranes in northern British Columbia are unconformably overlain by Upper Cretaceous volcanic, hypabyssal, and sedimentary rocks of the Montana Mountain complex and Windy-Table suite and cut by intrusive rocks of the Surprise Lake plutonic suite. Although these rocks are commonly spatially and temporally associated with mineral prospects, their regional distribution and inter-relationships are not well understood. Herein we present three new U-Pb zircon ages for Upper Cretaceous volcanic and plutonic rocks and new geochemical data. A sample of Peninsula Mountain rhyolite yielded a 85.0 ±1.6 Ma age indicating that it forms part of the Windy-Table suite. Mafic volcanic rocks previously assigned to Peninsula Mountain suite have the same geochemical characteristics as ophiolitic rocks of the Graham Inlet suite (Cache Creek terrane). These data indicate that the stratigraphy of the area requires significant revision. Ages from the Surprise Lake batholith of 79.70 ±0.15 Ma and from a granite near Tutshi Lake of 76.5 ±1.3 Ma are slightly younger than the Windy-Table suite volcanism. The age of these volcanic and plutonic rocks overlaps the age of magmatism and prolific mineralization in northern British Columbia and Yukon.

Keywords: Late Cretaceous magmatism, Windy-Table suite, Peninsula Mountain suite, Surprise Lake batholith, Graham Inlet suite, ophiolite

1. Introduction

The Cretaceous is a tectonically complex and economically important period in the development of the northern Cordilleran orogen. It marks the end of a high-flux magmatic episode (DeCelles et al., 2009) that led to the emplacement of mid-Cretaceous magmas throughout the Cordillera. Many workers have presumed a back-arc to arc setting for this episode (ca. 115-90 Ma: Hart et al., 2004) and thus for mineral deposits and prospects such as copper skarns of the Whitehorse Copper belt (108-112 Ma; Hart, 1996; Hart, 1997). This magmatic-metallogenic epoch is broadly coeval with the end of dextral transpression inboard of the Intermontane superterrane, and cessation of motion on faults such as the Teslin-Thibert-Kutcho fault (Fig. 1), which are thought to have accommodated major translations only until mid-Cretaceous (Gabrielse et al., 2006). Subsequent Late Cretaceous magmatism was characterized by emplacement of low volume stocks and minor volcanic eruptions in a presumed arc setting and is associated with economic mineralization in British Columbia, Yukon and Alaska (Allan et al., 2013; Nelson et al., 2013; Simmons et al., 2005; Smith and Arehart, 2010).

Upper Cretaceous rocks are common in northwestern British Columbia (Fig. 2; Mihalynuk et al., 1999; Simmons et al., 2005; Smith and Arehart, 2010) and Yukon (Hart and Pelletier, 1989). Although these rocks host many mineral prospects, their stratigraphy, age, and distribution have not been considered collectively since the work of Hart (1997). Herein we present new U-Pb geochronological and geochemical data from the Atlin and Tagish lakes area (Figs. 2, 3) and consider their stratigraphic, magmatic, and metallogenic implications.

2. Regional geology

Atlin and Tagish lakes are the principal physiographic features in the study area (Fig. 2). Areas surrounding these lakes are underlain by rocks of the Stikine and Cache Creek terranes (Fig. 1), parts of which have been the subject of systematic regional studies by various workers (Gwillim, 1901; Watson and Mathews, 1944; Aitken, 1959; Monger, 1975, 1977; Bultman, 1979; Lefebure and Gunning, 1988; Bloodgood et al., 1989; Bloodgood and Bellefontaine, 1990; Ash, 1994; Mihalynuk et al., 1999, 2003). Stikine terrane comprises Late Devonian to Early Permian and Middle Triassic to Early Jurassic volcanic arc successions that, in Atlin area, are represented by volcano-sedimentary rocks of the Stuhini Group (Upper Triassic), plutonic rocks of Stikine plutonic suite (Upper Triassic), volcanic rocks of the Hazelton Group (Lower Jurassic) and sedimentary rocks of the Laberge Group (Lower to Middle Jurassic, Fig. 2). Cache Creek terrane comprises a diverse assemblage of Carboniferous to Lower Jurassic rocks (e.g., Monger, 1975; Golding et al., 2016).

The oldest dated Cache Creek units are the Horsefeed Formation limestone (Carboniferous to Permian) and

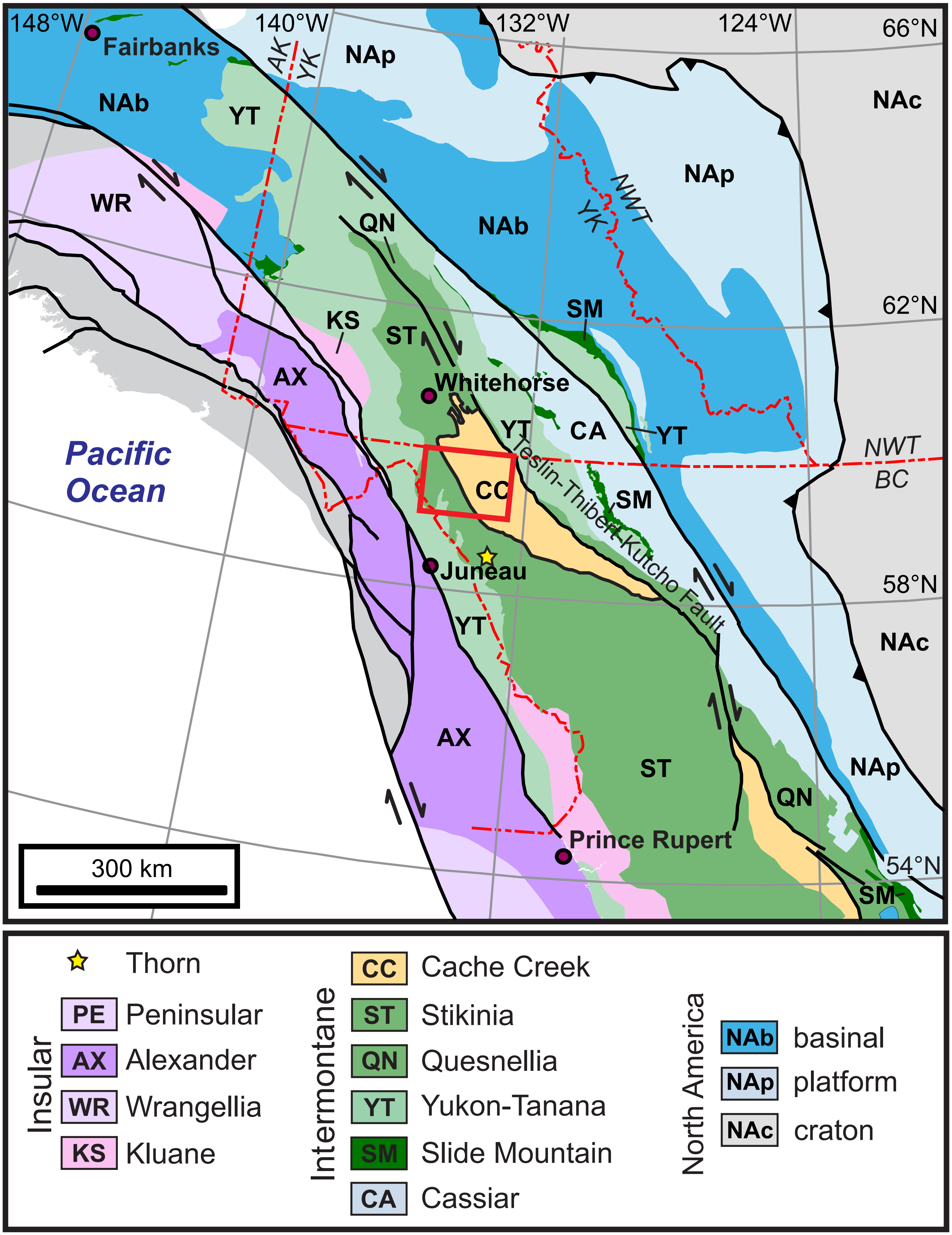

Fig. 1. Northern Cordillera terranes (from Colpron and Nelson, 2011). Atlin-Tagish Lake area outlined by solid red box.

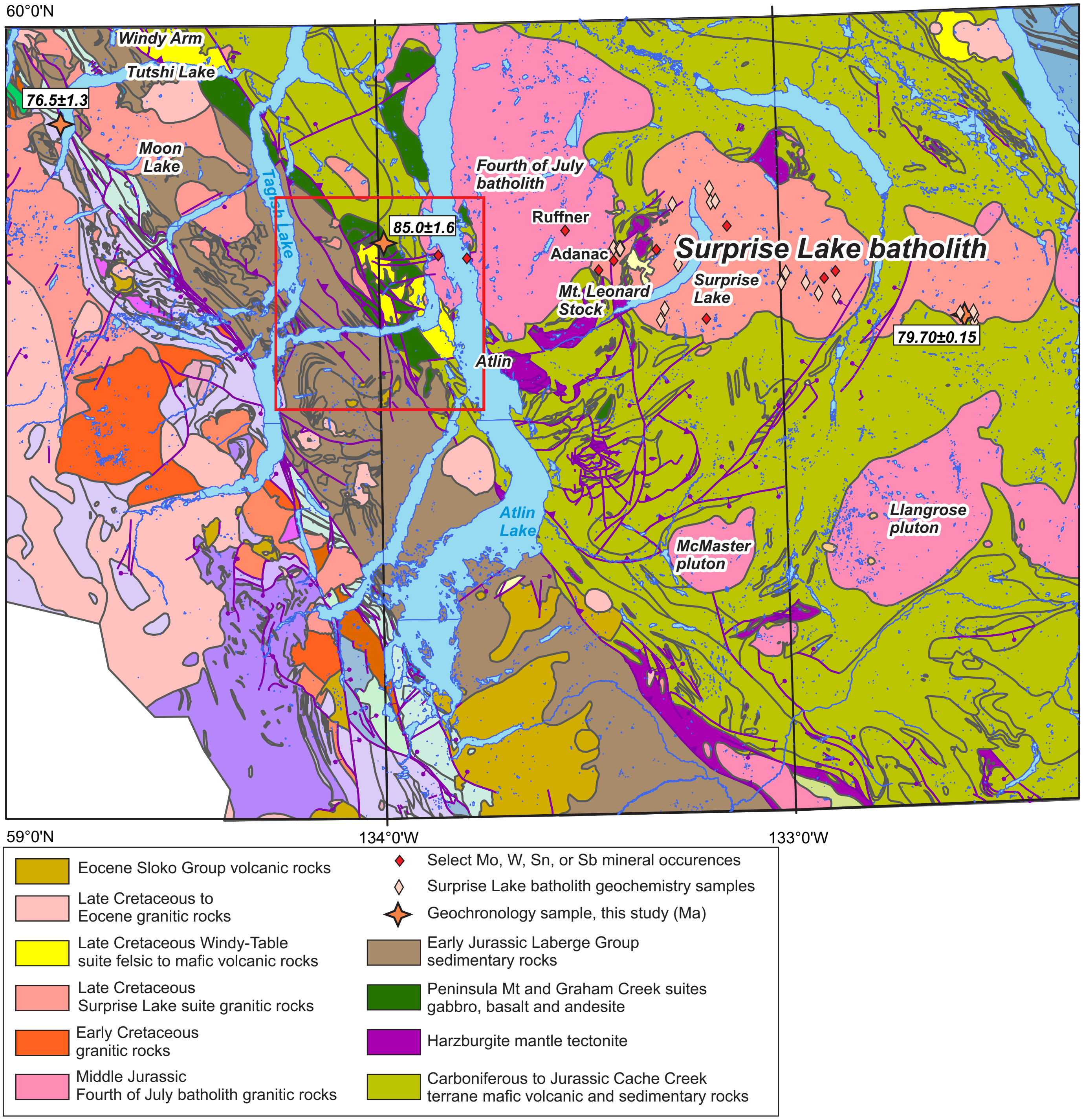

Fig. 2. Simplified geology of Atlin-Tagish Lake area (from Massey et al., 2005). Graham Inlet area outlined by solid red box.

siliciclastic rocks and chert of the Kedahda Formation (Early Carboniferous to Early Jurassic). Ophiolitic rocks once thought to form the basement of the terrane (e.g., Monger, 1975) are now known to be Upper Permian to Middle Triassic (Nakina formation, Graham Inlet suite, Peninsula Mountain suite, Mitchie Formation: Gordey et al., 1998; Mihalynuk et al., 1999, Mihalynuk et al., 2003; Bickerton et al., 2013). Triassic to Lower Jurassic siliciclastic and chemical sedimentary rocks once included in the Kedahda Formation have been recognized in some areas as a separate unit (Mihalynuk et al., 2003; Fig. 2). Stikine and Cache Creek terranes are juxtaposed along the Nahlin fault, which commonly places ophiolitic mantle on its eastern side against sedimentary rocks of the Laberge Group (Early to Middle Jurassic) to the west.

Stikine and Cache Creek terrane rocks were deformed, locally intensely, before emplacement of the Three Sisters plutonic

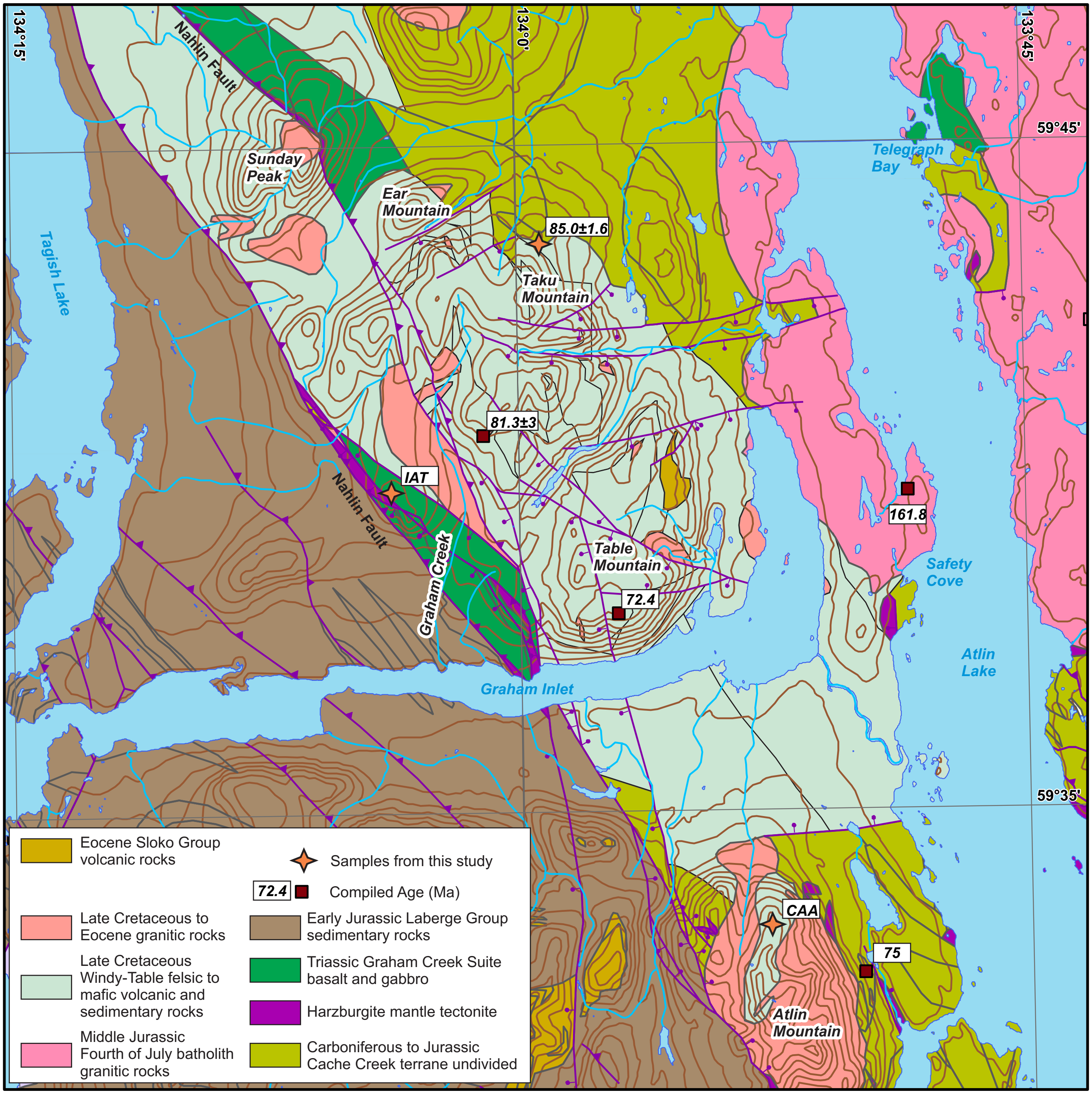

Fig. 3. Revised geology of the Graham Inlet area (modified from Massey et al., 2005) on the basis of new data. IAT- island arc tholeiite, CAA – calc-alkaline andesite. Ages from Breitsprecher and Mortensen (2004).

suite (Middle Jurassic). Intrusions belonging to this suite are the Fourth of July batholith, Llangorse and McMaster plutons and coeval satellite stocks, which intrude on both sides of the Nahlin fault and thermally metamorphose previously deformed rocks of the Cache Creek terrane and Whitehorse Trough (Fig. 2; ca. 172 Ma: Mihalynuk et al., 1992). A magmatic lull followed Three Sisters plutonic suite magmatism with low magmatic productivity lasting from ~165 to 115 Ma (Mihalynuk et al., 1999). Resumption of high-flux magmatism in the mid-Cretaceous is marked by emplacement of voluminous Coast Plutonic Complex intrusions to the west (Massey et al., 2005) and Whitehorse plutonic suite to the north of the study area (Colpron et al., 2016). Coeval volcanic strata are preserved in the lower part of the Montana Mountain complex (ca. 95 Ma: Hart, 1996). This episode was followed by deposition of volcano-sedimentary rocks in the upper part of the Montana Mountain complex and the Windy-Table suite (ca. 84 Ma: Hart, 1996; ca. 81 Ma: Mihalynuk et al., 1992), and emplacement of coeval plutonic rocks of the Surprise Lake plutonic suite and its correlatives (Fig. 2; ca. 83-78 Ma: Mihalynuk et al., 1992; Smith and Arehart, 2010).

2.1. Permian to Early Jurassic rocks

The Cache Creek terrane (Fig. 1) contains aerially extensive mafic-ultramafic ophiolitic rocks and overlying siliciclastic and chemical sedimentary rocks. Crustal ophiolitic rocks have been included in the Nakina Formation, Graham Inlet suite, and Peninsula Mountain suite (Late Permian to Middle Triassic: Mihalynuk et al., 1999, Mihalynuk et al., 2003). Triassic to Lower Jurassic siliciclastic and chemical sedimentary rocks of the Kedahda Formation (e.g., Golding et al., 2016) are locally interlayered with ophiolitic rocks but are generally mapped as a separate unit. In the study area, the Graham Creek suite contains ultramafic rocks, gabbro and tholeiitic pillow basalt (Mihalynuk et al., 1999). The Peninsula Mountain suite is inferred to overlie ophiolitic rocks of the Graham Creek suite. The Peninsula Mountain suite consists of conglomeratic rocks, pyritic rhyolite, calc-alkaline andesite breccia, polylithic breccia, pillow basalt, and interbedded chert and wacke (Mihalynuk et al., 1999).

2.2. Montana Mountain complex and older

Lower Cretaceous volcanic rocks are spatially restricted in northern British Columbia. Lower Cretaceous intermediate to felsic volcanic rocks were deposited paraconformably on Laberge Group (Jurassic) strata west of Tutshi Lake. These rocks yielded a 124.9 ±0.5 Ma crystallization age based on the two most-concordant zircon fractions (Mihalynuk et al., 2003). Deposition of these rocks was followed by deposition of the Montana Mountain complex, which at its type locality in Yukon, comprises two units separated by ca. 10 m.y. (Hart, 1996). The lower unit consists of green to maroon andesite and mafic flows that yielded a 95 ±1 Ma U-Pb zircon age (Hart, 1996). These are overlain by rhyolite flows, breccia and andesite that yielded a 84 ±1 Ma U-Pb zircon age (Hart, 1996). The Montana Mountain complex was interpreted by Mihalynuk et al. (1999) to extend from Yukon to Windy Arm. For the purposes of mapping and to retain consistency with BC nomenclature, Mihalynuk et al. (1999) used Montana Mountain complex for andesitic rocks at Windy Arm but assigned other felsic and andesitic rocks to the Windy-Table suite (see below).

2.3. Windy-Table suite

The Windy-Table suite (Mihalynuk et al., 1999: Hutshi Formation of Bultman, 1979) comprises andesite to rhyodacite flows and tuff, and minor basalt that are discontinuously exposed from Windy Arm to Atlin Mountain (Figs. 3, 4). The Windy-Table suite was deposited on Jurassic and older rocks in the area above an unconformity surface with more than a kilometre of relief (Bultman, 1979). At Table Mountain, felsic volcanic rocks near the top of the Windy-Table suite yielded a 81.3 ±0.3 Ma U-Pb zircon crystallization age (Mihalynuk et al., 1992).

2.4. Surprise Lake plutonic suite

The Surprise Lake plutonic suite (Late Cretaceous) consists of texturally heterogeneous biotite granites that form two aerially extensive bodies (Surprise Lake batholith), the Mount Leonard stock, and several small plutons west of Atlin Lake (Fig. 2; Aitken, 1959; Ballantyne and Littlejohn, 1982; Mihalynuk et al., 1999). The granites include irregularly distributed phases that are equigranular, seriate, megacrystic, or porphyritic. They commonly contain biotite, alkali feldspar, lesser plagioclase, and smokey quartz, although some zones are aplitic or pegmatitic with miarolitic cavities (Lowe et al., 2003). Mihalynuk et al. (1992) obtained a crystallization age of 83.8 ±5 Ma (U-Pb zircon) from the marginal phase of the Surprise Lake batholith southeast of Surprise Lake. Detailed study of the Mount Leonard stock, host to the Adanac molybdenum deposit east of Surprise Lake, yielded U-Pb age determinations ranging from 81.6 ±1.1 to 77.5 ±1.0 Ma, and significantly younger molybdenum Re/Os ages, from 70.87 ±0.36 to 69.72 ±0.35 Ma (Smith and Arehart, 2010), similar to previous K-Ar and Rb-Sr age determinations (Christopher and Pinsent, 1982; Mihalynuk et al., 1992). Coeval intrusions west of Atlin Lake, including the Racine and Atlin Mountain plutons, are compositionally distinctive, relatively homogeneous quartz diorite to granodiorite. All were included with what Mihalynuk et al. (1999) termed the 'Carmacks magmatic epoch', constrained mainly by cooling ages of ~85 to 70 Ma (mostly by Bultman, 1979).

3. U-Pb geochronology

We collected samples of granitic rocks from the Surprise Lake batholith (CL01-094) and from a pluton near Tutshi Lake (MMI15-18-3) and a sample of rhyolite from the Peninsula Mountain suite (ZE10-248). Zircon separates were prepared by standard crushing, disk mill, WilfleyTM table, and heavy liquid techniques. Mineral separates were sorted by magnetic susceptibility using a FrantzTM isodynamic separator.

For the Surprise Lake batholith sample, zircons were analyzed using U-Pb TIMS as outlined in Parrish et al. (1987). Multigrain zircon fractions analyzed were very strongly air abraded following the method of Krogh (1982). Treatment of analytical errors follows Roddick et al. (1987), with errors on the ages reported at the 2σ level (Table 1).

Zircons from samples ZE10-248 and MMI15-18-3 were analyzed on separate mounts using the Sensitive High Resolution Ion Microprobe (SHRIMP) at the Geological Survey of Canada in Ottawa. Analytical procedures and calibration details for the SHRIMP followed those described by Stern (1997) and Stern and Amelin (2003). Zircons were cast in 2.5 cm diameter epoxy mounts along with the Temora2 zircon primary standard, the accepted $^{206}Pb/^{238}U$ age of which is 416.8 ±0.33 Ma (Black et al., 2005). Fragments of the GSC laboratory zircon standard (z6266, with $^{206}Pb/^{238}U$ age = 559 Ma) were also included on the mounts as a secondary standard, analyses of which were interspersed among the sample analyses throughout the data sessions to verify the accuracy of the U-Pb calibration. The

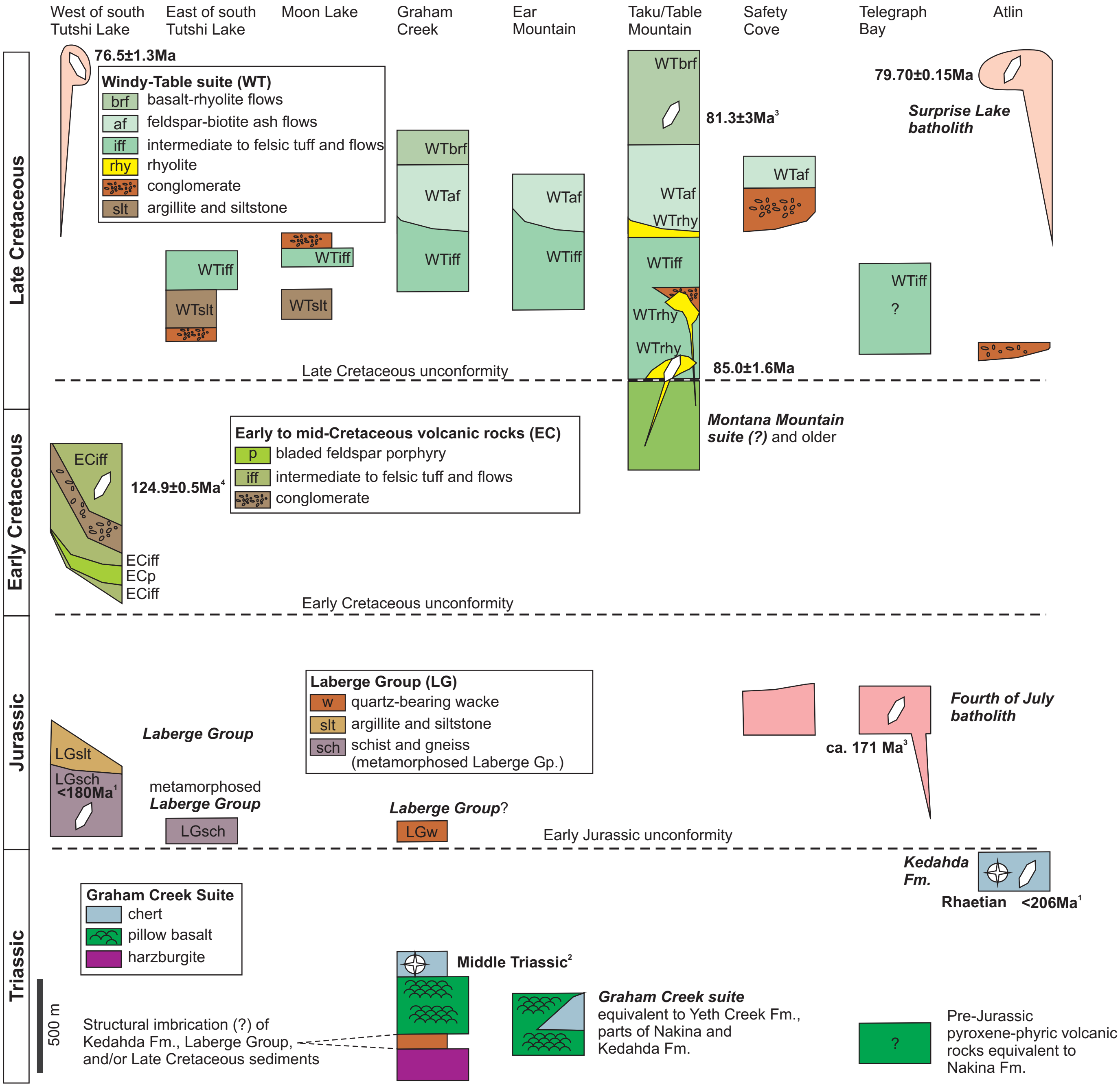

Fig. 4. Revised schematic stratigraphy of Triassic to Cretaceous rocks in the Atlin-Tagish area (modified from Mihalynuk et al., 1999). [1]Zagorevski, Joyce, and Cordey (unpublished data); [2]Mihalynuk et al.(1999); [3]Mihalynuk et al. (1992); [4] Mihalynuk et al. (2003).

mid-sections of the zircons were exposed using 9, 6, and 1 μm diamond compound, and internal features (e.g., zoning, structures, and alteration) were examined in both back-scattered electron mode (BSE) and cathodoluminescence mode (CL) using a Zeiss Evo 50 scanning electron microscope. The mount surfaces were evaporatively coated with 10 nm of high purity Au. Analyses were conducted during two separate data sessions, using an 16O- primary beam, projected onto the zircons at 10 kV. Before analysis, the ion beam was rastered over the area of interest for 2 minutes to remove the Au coating and eliminate effects of surface common lead. The sputtered area used for analysis was ca. 16 μm in diameter with beam currents of ~4 nA-7.5 nA. The count rates at ten masses including background were sequentially measured over 6 scans with a single electron multiplier and a pulse counting system with a deadtime of 11 ns (for sample ZE10-248) and 20 ns (for sample MMI15-18-3). The 1σ external errors of $^{206}Pb/^{238}U$ ratios reported in Table 2 incorporate a ±0.80 - 1.60% error in calibrating the standard Temora2 zircon. Age errors are at the 2σ uncertainty level, and encompass the combined statistical uncertainty of

Table 1. ID-TIMS U-Pb zircon geochronological data.

Fraction Descr. [12]	# Grains	Size µm	Wt ug	U ppm	Pb[3] ppm	206Pb[4]/204Pb	Pb[5] pg	208Pb/206Pb	207Pb/235U	±1SE Abs	206Pb/238U	±1SE Abs	Corr.[7] Coeff.	207Pb/206Pb	±1SE Abs	206Pb/238U	± 2SE	207Pb/235U	± 2SE	207Pb/206Pb	± 2SE	% Disc
						Isotopic Ratios[6]										Ages (Ma)[8]						
CL01-094 (Z7208): Surprise Lake batholith (granite) *08V 635587E 6611708N NAD 83*																						
Z1-El,Fg	43	74-200	52.0	404	5	1971	8.33	0.09875	0.081457	0.000199	0.012447	0.000022	0.624800	0.04746	0.00009	79.74	0.28	79.51	0.37	72.6	9.1	-10
Z2-El,Fg	82	<74	17.6	506	6	991.3	7.09	0.09990	0.082182	0.000360	0.012469	0.000027	0.433062	0.04780	0.00019	79.88	0.34	80.19	0.68	89.5	18.7	11
Z3-Eq,Fg,St	164	<74	50.6	584	7	2951	7.84	0.09811	0.082423	0.000133	0.012514	0.000014	0.807573	0.04777	0.00005	80.17	0.18	80.42	0.25	87.8	4.6	8.8
Z4-Eq,Fg,St	56	74-105	59.7	519	6	2883	8.36	0.09420	0.081802	0.000147	0.012426	0.000017	0.709603	0.04774	0.00006	79.61	0.21	79.84	0.28	86.6	6	8.1

[1]Z=zircon fraction; All fractions were air abraded following the method of Krogh (1982);[2]Zircon descriptions: all zircon fractions are abraded, colourless to pale yellow, with few clear to opaque inclusions from Frantz non-magnetic fraction at 0° sideslope and magnetic fraction at 0° sideslope, El=Elongate, Eq=Equant, Fg=Fragment, St=Stubby Prism;[3]Radiogenic Pb;[4]Measured ratio, corrected for spike and fractionation;[5]Total common Pb in analysis corrected for fractionation and spike;[6]Corrected for blank Pb and U and common Pb, errors quoted are 1 sigma absolute; procedural blank values for this study were from 0.1 pg U and 1 pg Pb for zircon analyses;[7]Correlation Coefficient;[8]Corrected for blank and common Pb, errors quoted are 2 sigma in Ma; The error on the calibration of the GSC 205Pb-233U-235U spike utilized in this study is 0.22% (2s).

the weighted mean age for the population and the 2σ error of the mean of the Temora2 zircon calibration standard. Off-line data processing was accomplished using customized in-house software. Isoplot v. 3.00 (Ludwig, 2003) was used to generate concordia plots and to calculate weighted means. Errors for isotopic ratios in Table 2 are given at 1σ uncertainty, as are the apparent SHRIMP ages. No fractionation correction was applied to the Pb-isotope data; common Pb correction used the Pb composition of the surface blank (Stern, 1997). All ages are reported as the ^{207}Pb-corrected weighted mean ^{206}Pb/^{238}U age. The error ellipses on the concordia diagrams and the weighted mean errors are reported at 2σ.

3.1. CL01-094 (Z7208) Surprise Lake batholith granite (79.70 ±0.15 Ma)

Sample CL01-094 is a biotite monzogranite to alkali-feldspar granite from the southern margin of the Surprise Lake batholith in the Snowdon Range (Fig. 2). Zircons from this sample are equant to stubby to elongate prisms 70-200 µm long. Most are euhedral to subhedral faceted prisms and fragments with square cross sections. In transmitted light, the crystals range from clear and colourless to pale yellow, with minor clear and opaque inclusions and fractures. Four fractions were analyzed, all of which overlap concordia (Fig. 5a, Table 1). Fraction Z3 comprises 164 equant to stubby prismatic grains and yields a ^{206}Pb/^{238}U age of 80.2 ±0.2 Ma. This is slightly older than the other three fractions, and is thus considered to reflect an inherited component. Fractions Z1, Z2, and Z3 consist of elongate, stubby prismatic to equant grains All three fractions overlap each other on concordia, and their weighted average ^{206}Pb/^{238}U age is 79.70 ±0.15 Ma (MSWD = 0.97, POF = 0.38). This is considered to be the crystallization age of the Surprise Lake batholith granite.

3.2. ZE10-248 (Z10297) Rhyolite northeast of Taku Mountain (85.0 ±1.6 Ma)

Sample ZE10-248 is from an altered, white to grey weathering, aphyric flow-banded rhyolite on the north side of Taku Mountain, previously included in the Peninsula Mountain suite (Mihalynuk et al., 1999). Most zircons from this sample are fragments of stubby to semi-elongate prisms 50-200 µm long, and are clear and colourless to pale yellow. Although most grain fragments have preserved facets, others are slightly rounded, with grain surfaces that are pitted and chipped. Fractures and clear bubble-shaped inclusions are common. SEM-CL images reveal two contrasting grain types (Fig. 5b). Type I zircons are bright in CL (relatively low U), with distinct oscillatory and/or sector-zoning. Type II zircons are dark grey in CL (relatively high U), and grains are either homogeneous and unzoned or oscillatory-zoned. In transmitted light, types I and II zircon are indistinguishable.

Type I grains have a broad range of low to high U content (105-594 ppm) and moderate Th/U (0.23-0.55). The weighted mean ^{207}Pb-corrected ^{206}Pb/^{238}U age of this sample is 174 ±2 Ma (n = 14, MSWD = 0.64; Fig. 5b). Type II zircon contain higher amounts of U (635-3491 ppm) and moderate Th/U (0.28-0.60). Nine Type II zircon grains yield a ^{207}Pb-corrected ^{206}Pb/^{238}U age of 85.0 ±1.6 Ma (n = 9, MSWD = 1.5; Fig. 5b). One analysis, spot 10297-9.1, yields an age of 146 Ma; this result is interpreted to record mixing of differently aged zircons and was excluded from age calculations and interpretations. The age from the type II zircon of 85.0 ±1.6 Ma is interpreted as the rhyolite crystallization age. Type I zircon grains are interpreted as inherited from the Fourth of July batholith or coeval rocks.

3.3. MMI15-18-3 (Z11799) biotite monzogranite near Tutshi Lake (76.5 ±1.3 Ma)

Sample MMI15-18-3 is from a medium-grained, K-feldspar porphyritic biotite monzogranite to alkali feldspar granite (Figs. 2 and 5c) from highway outcrops along the west shore of Tutshi Lake. This granite is chilled against deformed Laberge Group strata along the east shore of southern Tutshi Lake where it yielded a poor-quality K-Ar biotite age of ~80 Ma (Bultman, 1979; recalculated).

Zircons from this sample are large (125-300µm) euhedral stubby to elongate prisms. In transmitted light, the grains are clear and colourless, with abundant colourless bubble- and rod-shaped inclusions. In SEM-CL images, central regions of most grains exhibit sector-zoned or striped growth, mantled by igneous oscillatory-zoned zircon of varying thickness. The

Table 2. SHRIMP U-Pb zircon geochronological data.

Spot	U ppm	Th ppm	Th/U	$^{206}Pb^*$ ppm	$^{204}Pb/^{206}Pb$	±	f(206) %	$^{208*}Pb/^{206*}Pb$	±	$^{238}U/^{206}Pb$	±	$^{207}Pb/^{206}Pb$	±
ZE10-248 - Rhyolite (NAD83 Zone 8: 556929 E 6621288 N; Z10297; Mount IP579)													
Type II Zircon													
7.1	797	309	0.40	8.5	0.0001339	0.0001339	0.24	0.1140	0.0142	80.443	2.309	0.0452	0.0028
25.1	1612	467	0.30	18.0	0.0004022	0.0001520	0.73	0.0665	0.0091	76.550	1.238	0.0493	0.0017
21.1	635	368	0.60	7.1	0.0001176	0.0001176	0.21	0.2128	0.0171	76.201	1.497	0.0487	0.0025
32.1	648	343	0.55	7.3	0.0002715	0.0001920	0.49	0.1774	0.0177	75.662	1.415	0.0519	0.0028
11.1	2014	536	0.28	23.1	*bdl*		0.00	0.0883	0.0066	75.001	1.210	0.0497	0.0015
24.1	1328	386	0.30	15.1	0.0003711	0.0001515	0.67	0.0893	0.0100	75.167	1.334	0.0474	0.0018
2.1	1633	517	0.33	18.8	*bdl*		0.00	0.1027	0.0078	74.761	1.244	0.0489	0.0017
17.1	1420	428	0.31	16.4	0.0001253	0.0000886	0.23	0.0802	0.0085	74.210	1.203	0.0452	0.0018
15.1	3491	2013	0.60	41.1	0.0000834	0.0000401	0.15	0.1843	0.0063	72.854	1.180	0.0480	0.0010
9.1	1711	729	0.44	33.8	-0.000032	-0.000032	-0.06	0.1257	0.0066	43.553	0.71	0.0488	0.0013
Type I Zircon													
31.1	578	130	0.23	13.2	0.0002605	0.0001504	0.47	0.0631	0.0103	37.516	0.618	0.0490	0.0046
30.1	105	28	0.28	2.4	0.0004340	0.0004340	0.78	0.1159	0.0314	36.766	0.683	0.0589	0.0054
26.1	454	219	0.50	10.5	0.0000911	0.0000911	0.16	0.1453	0.0127	37.058	0.612	0.0514	0.0041
28.1	369	163	0.46	8.5	0.0002632	0.0001861	0.48	0.1367	0.0162	36.998	0.618	0.0496	0.0027
23.1	396	195	0.51	9.2	*bdl*		0.00	0.1435	0.0132	36.783	0.646	0.0513	0.0025
20.1	525	270	0.53	12.2	0.0000819	0.0000819	0.15	0.1825	0.0135	36.936	0.607	0.0476	0.0020
19.1	169	56	0.34	3.9	0.0006648	0.0003839	1.20	0.0744	0.0215	36.751	0.855	0.0504	0.0035
29.1	274	145	0.55	6.4	0.0008911	0.0003986	1.61	0.1561	0.0241	36.331	0.717	0.0567	0.0033
16.1	138	50	0.38	3.2	0.0008055	0.0004652	1.45	0.0949	0.0258	36.695	0.777	0.0455	0.0037
18.1	313	136	0.45	7.4	*bdl*		0.00	0.1495	0.0142	36.403	0.607	0.0507	0.0025
27.1	452	225	0.51	10.7	0.0005190	0.0002119	0.94	0.1478	0.0148	35.929	0.686	0.0554	0.0022
14.1	407	172	0.44	9.6	0.0003908	0.0001954	0.71	0.1194	0.0207	35.994	0.594	0.0494	0.0039
13.1	203	105	0.53	4.8	0.0007214	0.0004166	1.30	0.0913	0.0231	35.628	0.909	0.0516	0.0037
19.2	594	174	0.30	14.3	0.0002626	0.0001313	0.47	0.0941	0.0097	35.486	0.619	0.0535	0.0033
MMI15-18-3 - Granodiorite (NAD83 Zone 8: 511777 E 6634078 N; Z11799; Mount IP824)													
6.1	294	111	0.39	3.0	0.0002032	0.0001437	0.35	0.1366	0.0138	85.133	1.299	0.0513	0.0020
34.1	206	106	0.53	2.1	0.0004876	0.0002816	0.85	0.1619	0.0209	84.883	2.845	0.0537	0.0027
7.1	150	58	0.40	1.5	0.0004128	0.0002920	0.72	0.1229	0.0206	85.186	1.863	0.0463	0.0028
16.1	415	196	0.49	4.2	0.0002220	0.0001282	0.38	0.1288	0.0113	85.107	0.887	0.0466	0.0016
32.1	557	475	0.88	5.6	0.0003115	0.0001393	0.54	0.2926	0.0156	84.887	1.232	0.0468	0.0016
10.1	295	104	0.36	3.0	0.0006008	0.0002454	1.04	0.1096	0.0150	84.694	0.787	0.0474	0.0019
2.1	168	59	0.36	1.7	*bdl*		0.00	0.1160	0.0156	84.979	2.371	0.0442	0.0025
9.1	407	190	0.48	4.1	0.0001542	0.0001091	0.27	0.1561	0.0124	84.370	1.320	0.0489	0.0017
3.1	345	197	0.59	3.5	0.0004334	0.0001939	0.75	0.1811	0.0157	83.686	1.910	0.0518	0.0019
1.1	328	207	0.65	3.3	0.0005748	0.0002348	1.00	0.1912	0.0170	84.117	0.758	0.0467	0.0018
38.1	267	115	0.45	2.7	0.0004778	0.0002390	0.83	0.1211	0.0162	83.737	1.477	0.0476	0.0021
4.1	202	112	0.57	2.1	0.0004122	0.0002381	0.71	0.1488	0.0177	83.527	1.975	0.0461	0.0023
8.1	168	66	0.40	1.8	-0.000358	-0.000253	-0.62	0.1240	0.0173	82.815	1.638	0.0477	0.0026
31.1	352	154	0.45	3.7	-0.000269	-0.000156	-0.47	0.1450	0.0128	82.844	1.884	0.0457	0.0018
17.1	370	174	0.49	3.9	-0.000155	-0.000109	-0.27	0.1645	0.0121	82.252	1.163	0.0474	0.0017
18.1	322	200	0.64	3.4	0.0002998	0.0001731	0.52	0.1736	0.0158	81.979	0.748	0.0474	0.0019
33.1	395	209	0.55	4.2	0.0002263	0.0001307	0.39	0.1808	0.0134	81.207	1.181	0.0459	0.0016

Notes (see Stern, 1997): Mount IP579, K100b spot size (13x16μm), 2 minute raster, 6 mass scans, Primary beam intensity ~4nA; weighted mean ^{207}Pb-corrected $^{206}Pb/^{238}U$ age of secondary standard z6266 zircon was 569 ± 6 Ma, MSWD=0.56, n=25 (2 rejections); error in $^{206}Pb/^{238}U$ calibration 1.60% (included). Standard Error in Standard calibration was 0.42% (not included in above errors). Mount IP824, K100b spot size (13x16μm), 2 minute raster, 6 mass scans; Primary beam intensity ~7.5nA; Weighted mean ^{207}Pb-corrected $^{206}Pb/^{23}8U$ age of secondary standard z6266 zircon was 558 ± 8 Ma, MSWD=1.4, n=25 (2 rejections) (accepted $^{206}Pb/^{238}U$ age is 559 Ma); Error in $^{206}Pb/^{238}U$ calibration 0.80% (included); Standard Error in Standard calibration was 0.72% (not included in above errors).

Table 2. Continued.

Spot	$^{207*}Pb/^{235}U$	±	$^{206*}Pb/^{238}U$	±	Corr Coeff	$^{207*}Pb/^{206*}Pb$	±	$^{206}Pb/^{238}U$ apparent age (Ma) 204 corrected Age	±	207 corrected Age	±
ZE10-248											
Type II Zircon											
7.1	0.074	0.006	0.0124	0.0004	0.344	0.0432	0.0034	79.5	2.3	**79.9**	**2.3**
25.1	0.078	0.005	0.0130	0.0002	0.241	0.0434	0.0029	83.1	1.4	**83.5**	**1.4**
21.1	0.085	0.006	0.0131	0.0003	0.292	0.0470	0.0030	83.9	1.6	**83.9**	**1.7**
32.1	0.087	0.007	0.0132	0.0003	0.224	0.0479	0.0040	84.2	1.6	**84.2**	**1.6**
11.1	0.091	0.003	0.0133	0.0002	0.463	0.0497	0.0015	85.4	1.4	**85.2**	**1.4**
24.1	0.076	0.005	0.0132	0.0002	0.251	0.0419	0.0029	84.6	1.5	**85.2**	**1.5**
2.1	0.090	0.003	0.0134	0.0002	0.436	0.0489	0.0017	85.7	1.4	**85.5**	**1.4**
17.1	0.080	0.004	0.0134	0.0002	0.301	0.0433	0.0022	86.1	1.4	**86.6**	**1.4**
15.1	0.088	0.003	0.0137	0.0002	0.550	0.0468	0.0011	87.8	1.4	**87.9**	**1.4**
9.1	0.156	0.005	0.0230	0.0004	0.505	0.0493	0.0014	146.4	2.4	146.4	2.4
Type I Zircon											
31.1	0.165	0.019	0.0265	0.0004	0.145	0.0452	0.0052	168.8	2.8	**169.7**	**2.9**
30.1	0.195	0.032	0.0270	0.0005	0.125	0.0525	0.0084	171.7	3.4	**171.0**	**3.4**
26.1	0.186	0.016	0.0269	0.0004	0.190	0.0501	0.0043	171.4	2.8	**171.3**	**2.9**
28.1	0.170	0.015	0.0269	0.0005	0.198	0.0457	0.0039	171.1	2.9	**171.9**	**2.9**
23.1	0.192	0.010	0.0272	0.0005	0.336	0.0513	0.0025	172.9	3.0	**172.5**	**3.0**
20.1	0.173	0.009	0.0270	0.0004	0.309	0.0464	0.0024	172.0	2.8	**172.6**	**2.8**
19.1	0.150	0.025	0.0269	0.0007	0.143	0.0405	0.0068	171.0	4.1	**172.9**	**4.1**
29.1	0.163	0.026	0.0271	0.0006	0.132	0.0436	0.0069	172.3	3.6	**173.5**	**3.5**
16.1	0.124	0.030	0.0269	0.0006	0.095	0.0335	0.0080	170.8	3.8	**174.2**	**3.7**
18.1	0.192	0.010	0.0275	0.0005	0.318	0.0507	0.0025	174.7	2.9	**174.5**	**2.9**
27.1	0.181	0.015	0.0276	0.0005	0.233	0.0477	0.0039	175.3	3.4	**175.7**	**3.4**
14.1	0.166	0.019	0.0276	0.0005	0.150	0.0436	0.0049	175.4	2.9	**176.7**	**3.0**
13.1	0.156	0.028	0.0277	0.0007	0.147	0.0409	0.0073	176.2	4.6	**178.0**	**4.6**
19.2	0.192	0.015	0.0280	0.0005	0.222	0.0497	0.0038	178.3	3.1	**178.3**	**3.2**
MMI15-18-3											
6.1	0.078	0.005	0.0117	0.0002	0.2	0.0484	0.0029	75.0	1	**74.9**	**1.2**
34.1	0.075	0.008	0.0117	0.0004	0.3	0.0466	0.0050	74.9	3	**74.9**	**2.5**
7.1	0.065	0.008	0.0117	0.0003	0.2	0.0402	0.0052	74.7	2	**75.3**	**1.7**
16.1	0.070	0.004	0.0117	0.0001	0.2	0.0434	0.0025	75.0	0.8	**75.4**	**0.8**
32.1	0.068	0.004	0.0117	0.0002	0.2	0.0422	0.0026	75.1	1	**75.6**	**1.1**
10.1	0.062	0.007	0.0117	0.0001	0.1	0.0385	0.0042	74.9	0.8	**75.7**	**0.7**
2.1	0.072	0.005	0.0118	0.0003	0.4	0.0442	0.0025	75.4	2	**75.7**	**2.1**
9.1	0.076	0.004	0.0118	0.0002	0.3	0.0467	0.0024	75.8	1	**75.8**	**1.2**
3.1	0.074	0.006	0.0119	0.0003	0.3	0.0454	0.0034	76.0	2	**76.2**	**1.7**
1.1	0.062	0.006	0.0118	0.0001	0.1	0.0381	0.0040	75.4	0.7	**76.3**	**0.7**
38.1	0.066	0.007	0.0118	0.0002	0.2	0.0405	0.0041	75.9	1	**76.5**	**1.4**
4.1	0.066	0.007	0.0119	0.0003	0.2	0.0400	0.0042	76.2	2	**76.8**	**1.8**
8.1	0.089	0.008	0.0122	0.0002	0.2	0.0529	0.0045	77.9	2	**77.4**	**1.5**
31.1	0.083	0.005	0.0121	0.0003	0.4	0.0496	0.0029	77.7	2	**77.5**	**1.8**
17.1	0.083	0.004	0.0122	0.0002	0.3	0.0497	0.0023	78.1	1	**77.9**	**1.1**
18.1	0.072	0.005	0.0121	0.0001	0.1	0.0429	0.0032	77.8	0.7	**78.2**	**0.7**
33.1	0.072	0.004	0.0123	0.0002	0.2	0.0426	0.0025	78.6	1	**79.1**	**1.2**

Notes (continued): Calibration standard Temora2 age = 416.8 +/-0.33 Ma (Black et al., 2004). Uncertainties reported at 1s and are calculated by using SQUID 2.50.11.10.15, rev. 15 Oct 2011. f(206) refers to mole percent of total ^{206}Pb that is due to common Pb, calculated using the ^{204}Pb-method; common Pb composition used is the surface blank (4/6: 0.05770; 7/6: 0.89500; 8/6: 2.13840). * refers to radiogenic Pb (corrected for common Pb). Ages in bold are used in weighted mean age. bdl: below detection limit

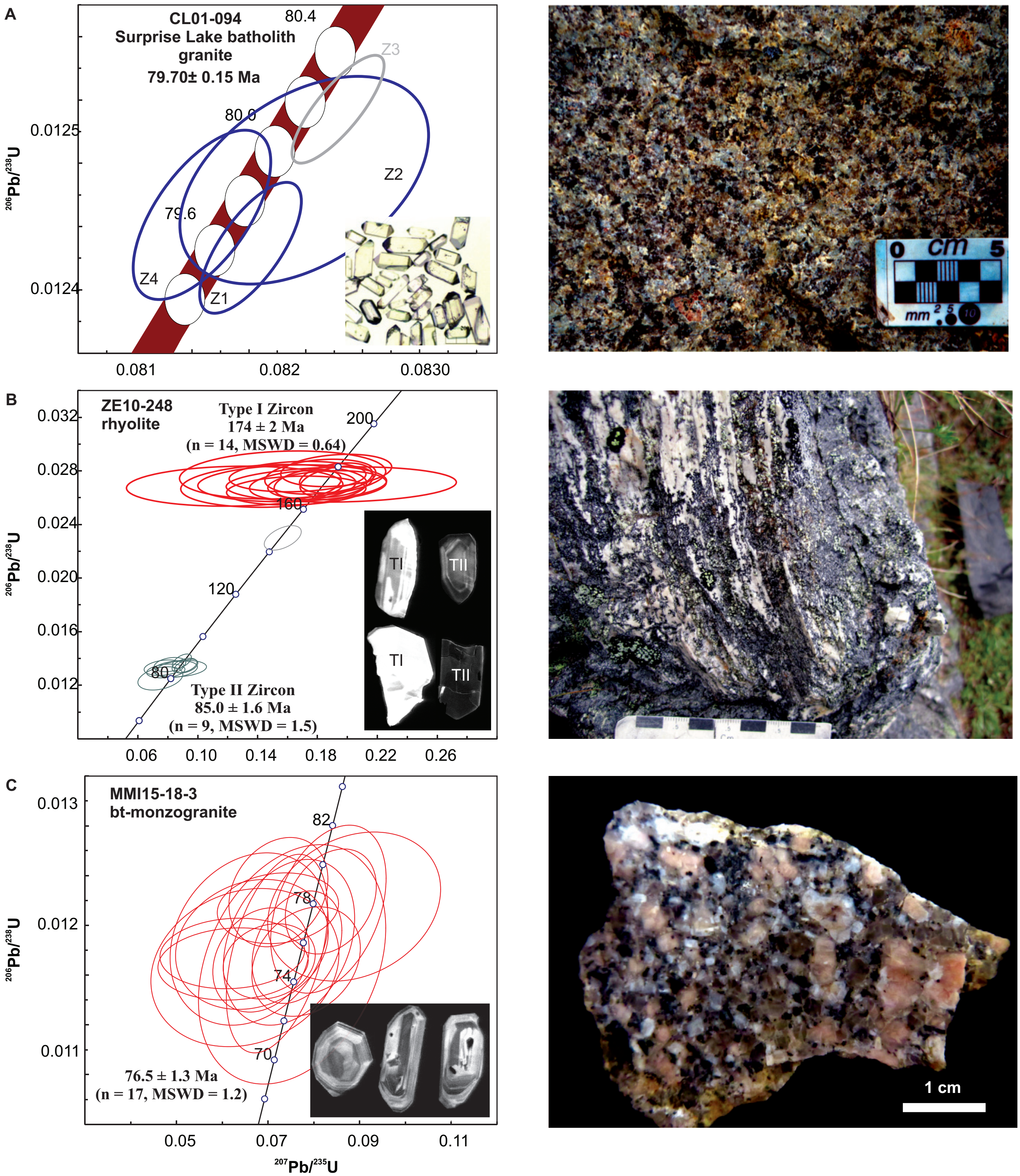

Fig. 5. U-Pb zircon concordia diagrams and representative photographs of Late Cretaceous samples. **a)** Surprise Lake batholith biotite alkali-feldspar granite. **b)** Rhyolite northeast of Taku Mountain. **c)** Biotite monzogranite near Tutshi Lake.

grains have a broad range of low to high U content (150-557 ppm) and moderate Th/U (0.36-0.88). The weighted mean ^{207}Pb-corrected ^{206}Pb/^{238}U age of this sample is 76.5 ±1.3 Ma (n = 17, MSWD = 1.2; Fig. 5c) and is interpreted as the crystallization age of the intrusion.

4. Geochemistry

Previously published whole-rock geochemical analyses of Mesozoic plutonic rocks in the Atlin map are either incomplete analyses or summary data (White et al., 1976; Ballantyne and Littlejohn, 1982; Mihalynuk et al., 1992, 1999; Ray et al., 2000). Twenty eight Surprise Lake batholith samples collected by Lowe et al. (2003) were analyzed at the Geological Survey of Canada (Ottawa, ON) for whole-rock major and trace element compositions (2002-2003; Table 3). Pulverized samples were mixed with a flux of lithium metaborate, fused, and dissolved using four acid digestions. The concentration of major elements was measured using x-ray fluorescence (XRF) on fused disks. For trace elements and rare-earth elements, samples were dissolved using four acid digestion followed by lithium metaborate fusion of the residue. Select trace elements (Ba, Be, Co, Cr, Cu, Ni, Sc, Sr, V and Zn) were measured by inductively coupled plasma-optical emission spectrometry (ICP-OES). The remaining trace elements, including rare earth elements (REE), were determined by inductively coupled plasma-mass spectrometry (ICP-MS). The uncertainty in measurement relative to concentration is <1% relative for major elements. The uncertainty in most trace and rare earth element concentrations measured by ICP-OES and ICP-MS is <10% relative. An additional 2 samples were collected during regional reconnaissance mapping in 2010 and analysed at Activation Laboratories (Ancaster, ON; using the 4Lithores analytical package, see Milidragovic et al. (2016) for analytical procedure and uncertainties).

The Surprise Lake batholith samples display high SiO_2 (average 73.43 wt.%) and K_2O (average 5.37 wt.%) and, on the basis of geochemistry are classified as alkali-feldspar granite to syenogranite (equivalent to rhyolite; Fig. 6a) typical of highly fractionated or minimum granitic melts generated in post-orogenic and anorogenic settings (Whalen and Frost, 2013). These samples are generally peraluminous and corundum normative (Fig. 6b), and plot in the alkalic to alkali-calcic fields on modified alkali-lime index (MALI) plots (Fig. 6c). On tectonic discrimination diagrams, Surprise Lake plutonic suite samples plot in within-plate granite fields (Fig. 6d). On MORB and chondrite-normalized REE and extended trace element and REE plots, the samples show significant Ba, Sr, Eu depletion indicative of plagioclase fractionation, and are highly enriched in Cs, Rb, Th, U and Pb (Figs. 6e, f).

Two samples of volcanic rocks were sampled from Peninsula Mountain suite of Mihalynuk et al. (1999). A sample of basalt was collected west of Graham Creek, from Peninsula Mountain suite pillow basalt sequence immediately adjacent to the Graham Creek suite (Fig. 3). The basalt (52.48 wt.% SiO_2) contains relatively high TiO_2 (1.35 wt.%) and displays a flat, MORB-like REE profile on an extended trace element plot, with slight Nb depletion and Th enrichment (Fig. 7b). It plots on the boundary between volcanic arc tholeiite, back-arc basin basalt, and normal mid-ocean ridge on a tectonic discrimination diagram (Fig. 7c). A sample of andesite was sampled from the Peninsula Mountain suite andesite sequence on the north side of Atlin Mountain (Fig. 3). The andesite (61.56 wt.% SiO_2, Fig. 7a) is enriched in Th, Ba, Sr, Pb, LREE and depeted in Nb, Ti and P on an extended N-MORB normalized trace element plot (Fig. 7d). It plots in calc-alkaline field on a Y-La-Nb tectonic discrimination diagram (Fig. 7c).

5. Discussion

Previous mapping in the area identified several Triassic to Cretaceous lithostratigraphic units (Bultman, 1979; Mihalynuk et al., 1999). Paucity of distinctive lithological characteristics, and general lack of age and geochemical constraints necessitated several revisions to the stratigraphy as new data became available, including reassignments of rocks between the Peninsula Mountain and Windy-Table suites and their equivalents (Mihalynuk et al., 1999). Data presented herein necessitate further revisions and indicate that Late Cretaceous magmatism and sedimentation are more widespread than previously thought. In particular, voluminous plutons east of Atlin have extensive volcanic and hypabyssal equivalents west of Atlin Lake (Fig. 2).

5.1. Peninsula Mountain suite

Rhyolite from the base of the Peninsula Mountain suite yielded a Late Cretaceous age (Fig. 5b), indicating that Peninsula Mountain suite to the north of Taku Mountain is actually part of the Windy-Table suite. This implies that andesitic rocks that appear to stratigraphically overlie the rhyolites must also form part of the Late Cretaceous supracrustal sequence (Figs. 3, 4). Whole-rock geochemical analyses from the andesitic and rhyolitic rocks (Mihalynuk et al., 1999) indicate strong LREE enrichment relative to MORB. Andesite on the northern flank of Atlin Mountain yields a similar LREE enrichment and is also likely part of the Windy-Table suite (Fig. 3).

Peninsula Mountain suite pillow basalts west of Graham Creek display a geochemistry that differs from other Peninsula Mountain suite volcanic rocks (Fig. 7) but is identical to the Graham Creek suite (Triassic). These are back-arc tholeiites with flat, MORB-like REE profile (Fig. 7b). However, our new data indicate that these rocks are not MORBs but rather back-arc basin basalts or primitive island arc tholeiites. Although Mihalynuk et al. (1999) noted that these rocks were distinctly different than the Cache Creek terrane, subsequent work demonstrated that island arc and bac-arc tholeiite geochemical signatures are characteristic of both the Nakina and Yeth Creek formations (Fig. 7b; English et al., 2010) in the Cache Creek terrane. As such, this pillow basalt is more appropriately included in the Graham Creek suite (Figs. 3, 4), and likely marks the western limit of the Cache Creek terrane.

Table 3. Whole rock geochemistry of Late Cretaceous rocks.

Sample	CL-01-94	AT02-01-01A	AT02-01-03A	AT02-02-02A	AT02-02-04A	AT02-02-05A	AT02-12-01A	AT02-12-02A	AT02-12-04A	AT02-14-07A
Laboratory	GSC	GSC	GSC	GSC	GSC	GSC	GSC	GSC	GSC	GSC
Latitude	59.6217	59.6166	59.6184	59.6055	59.6151	59.6191	59.7103	59.7078	59.7008	59.6626
Longitude	-132.5942	-132.5546	-132.5554	-132.5208	-132.5197	-132.5224	-132.8591	-132.8790	-132.8776	-132.9388
Rocktype	granite	granite	granite	granite	granite	granite	granite	granite	granite	granite
SiO2	77.30	74.70	74.60	71.50	72.90	72.70	72.50	72.80	73.20	72.50
Al2O3	11.80	13.40	13.30	14.50	14.30	14.30	14.40	14.00	14.00	14.30
Fe2O3(T)	1.40	1.40	1.10	1.10	1.70	1.30	1.50	2.00	1.70	1.90
MnO	0.01	0.01	0.01	0.01	0.02	0.01	0.01	0.04	0.01	0.02
MgO	0.10	0.06	0.05	0.03	0.08	0.07	0.07	0.23	0.07	0.03
CaO	0.40	0.65	0.70	0.84	0.66	0.75	0.70	1.05	0.73	0.66
Na2O	3.10	3.70	3.90	4.70	4.00	3.80	4.30	4.10	4.10	4.30
K2O	4.86	5.77	5.01	5.27	5.69	5.48	5.55	5.52	5.29	5.19
TiO2	0.08	0.11	0.12	0.21	0.16	0.17	0.14	0.21	0.14	0.10
P2O5	0.01	0.01	0.01	0.00	0.01	0.01	0.01	0.05	0.01	0.00
LOI	0.5	0.4	0.6	0.5	0.4	0.8	0.6	0.3	0.5	0.5
Total	99.8	100.2	99.5	98.7	100.0	99.5	99.9	100.5	99.7	99.5
Ba	260	213	159	73	273	142	119	336	127	62
Be	5.0	7.8	5.4	7.3	6.9	5.5	13.0	9.1	7.3	5.1
Cr	35	22	22	20	26	21	25	26	25	19
Cs	10.00	17.00	14.00	14.00	11.00	13.00	18.00	7.20	16.00	16.00
Ga	25.00	28.00	30.00	39.00	30.00	36.00	30.00	23.00	31.00	37.00
Hf	8.00	10.00	10.00	12.00	12.00	15.00	12.00	8.90	12.00	10.00
Mo	0.7	0.9	0.3	1.7	0.4	1.3	0.2	0.8	0.3	1.0
Nb	34.00	53.00	51.00	92.00	44.00	45.00	43.00	46.00	47.00	88.00
Pb	21	24	20	38	25	15	28	20	29	23
Rb	240	397	406	488	357	546	492	435	578	680
Sb	0.2	0.7	0.4	0.9	0.4	0.6	1.5	0.4	0.5	0.2
Sc	3.0	2.5	2.6	2.5	3.5	2.9	2.0	1.8	2.1	2.5
Sn	4.5	5.7	5.8	4.9	2.9	22.0	5.0	6.0	4.3	3.5
Sr	15	20	12	-10	27	-10	11	52	11	-10
Ta	4.30	5.50	5.80	8.80	4.30	5.00	5.50	7.00	7.80	16.00
Th	38.00	50.00	49.00	76.00	50.00	42.00	60.00	56.00	65.00	76.00
U	13.00	18.00	20.00	39.00	18.00	13.00	20.00	21.00	17.00	16.00
Y	73.00	99.00	113.00	220.00	64.00	163.00	110.00	69.00	196.00	217.00
Zr	183.0	250.0	213.0	195.0	309.0	358.0	284.0	235.0	251.0	185.0
La	73.0	89.0	70.0	49.0	113.0	93.0	74.0	59.0	122.0	65.0
Ce	164.0	184.0	140.0	130.0	274.0	202.0	154.0	118.0	196.0	146.0
Pr	16.00	21.00	18.00	15.00	26.00	24.00	17.00	12.00	29.00	18.00
Nd	58.0	73.0	64.0	57.0	88.0	87.0	59.0	38.0	102.0	67.0
Sm	11.00	16.00	15.00	18.00	17.00	21.00	14.00	7.70	25.00	20.00
Eu	0.19	0.20	0.14	0.05	0.22	0.11	0.11	0.34	0.13	0.04
Gd	10.00	15.00	15.00	22.00	13.00	21.00	14.00	6.90	26.00	22.00
Tb	1.90	2.70	2.70	4.40	2.10	3.80	2.70	1.30	4.90	4.70
Dy	11.00	17.00	17.00	29.00	12.00	23.00	17.00	8.50	30.00	32.00
Ho	2.20	3.40	3.70	6.50	2.40	5.10	3.70	1.90	6.50	7.00
Er	5.70	9.60	11.00	19.00	6.30	14.00	11.00	6.10	18.00	21.00
Tm	1.00	1.60	1.80	3.30	1.00	2.40	1.80	1.20	3.10	3.60
Yb	6.60	10.00	12.00	22.00	6.60	16.00	12.00	8.90	20.00	24.00
Lu	0.97	1.60	1.80	3.40	1.00	2.40	1.80	1.40	3.00	3.60

Table 3. Continued.

Sample	AT02-15-01A	AT02-15-04A	AT02-15-05A	AT02-16-03A	AT02-17-01A	AT02-17-06A	AT02-18-01A	AT02-18-03A	AT02-19-01A	AT02-19-01B
Laboratory	GSC	GSC	GSC	GSC	GSC	GSC	GSC	GSC	GSC	GSC
Latitude	59.7859	59.7683	59.7692	59.7666	59.6908	59.7185	59.6351	59.6206	59.7117	59.7117
Longitude	-133.1737	-133.1707	-133.1591	-133.2674	-133.2569	-133.2526	-133.2925	-133.3038	-133.4027	-133.4027
Rocktype	granite	granite	granite	granite	granite	granite	granite	granite	granite	granite
SiO2	73.20	72.20	75.00	73.10	71.20	74.90	72.70	73.20	73.10	73.50
Al2O3	14.40	14.40	13.60	14.80	14.80	14.10	14.60	14.40	13.40	12.90
Fe2O3(T)	1.70	1.30	1.10	1.30	1.70	0.60	1.20	1.40	1.90	2.40
MnO	0.05	0.02	0.01	0.01	0.02	0.00	0.04	0.02	0.05	0.04
MgO	0.22	0.10	0.09	0.07	0.06	0.17	0.14	0.06	0.35	0.28
CaO	1.00	0.97	0.95	0.30	0.81	0.08	0.83	0.65	1.02	0.82
Na2O	4.40	4.50	4.30	4.90	4.40	2.70	4.50	4.40	3.30	2.90
K2O	4.95	5.22	4.54	5.25	5.10	5.45	5.35	5.51	6.08	6.68
TiO2	0.18	0.12	0.10	0.07	0.10	0.16	0.11	0.13	0.20	0.17
P2O5	0.05	0.01	0.01	0.00	0.00	0.01	0.03	0.01	0.06	0.05
LOI	0.5	0.5	0.2	0.5	0.7	1.6	0.3	0.3	0.5	0.4
Total	100.6	99.4	100.1	100.3	98.8	99.8	99.9	100.1	100.0	100.3
Ba	355	205	200	126	99	1010	392	406	423	447
Be	10.0	10.0	8.1	16.0	5.6	2.9	6.7	6.4	8.9	7.5
Cr	25	24	23	21	22	20	30	28	20	27
Cs	16.00	11.00	5.70	18.00	26.00	4.40	6.00	7.10	5.00	5.70
Ga	21.00	31.00	25.00	32.00	38.00	17.00	21.00	30.00	20.00	20.00
Hf	7.10	11.00	11.00	13.00	12.00	4.70	5.70	8.10	5.60	4.90
Mo	0.4	0.3	0.5	0.2	1.4	2.0	0.2	0.3	47.0	101.0
Nb	39.00	81.00	40.00	56.00	80.00	28.00	31.00	42.00	54.00	46.00
Pb	25	37	31	35	17	161	28	30	17	20
Rb	404	611	272	645	731	282	361	291	342	399
Sb	0.4	0.2	0.4	0.7	1.0	0.8	-0.2	0.4	0.3	-0.2
Sc	1.6	1.8	1.3	1.9	3.5	1.6	1.7	2.0	2.3	2.0
Sn	11.0	3.2	3.5	2.0	9.8	2.8	5.4	6.3	5.2	5.7
Sr	64	33	33	11	-10	71	61	33	107	102
Ta	4.50	12.00	3.80	9.60	14.00	3.40	3.80	3.00	7.60	7.40
Th	55.00	74.00	66.00	88.00	73.00	16.00	44.00	40.00	42.00	41.00
U	17.00	35.00	16.00	22.00	18.00	3.50	12.00	12.00	17.00	22.00
Y	40.00	193.00	91.00	113.00	216.00	8.30	54.00	91.00	42.00	38.00
Zr	219.0	200.0	216.0	230.0	199.0	151.0	167.0	186.0	169.0	145.0
La	53.0	55.0	38.0	65.0	53.0	19.0	43.0	46.0	32.0	37.0
Ce	98.0	125.0	83.0	102.0	120.0	31.0	83.0	99.0	64.0	67.0
Pr	10.00	16.00	10.00	17.00	16.00	3.10	9.00	12.00	7.40	7.10
Nd	32.0	57.0	37.0	57.0	61.0	9.7	30.0	47.0	26.0	23.0
Sm	5.90	17.00	10.00	14.00	19.00	1.80	6.40	13.00	5.20	4.70
Eu	0.37	0.16	0.20	0.09	0.07	0.23	0.32	0.31	0.41	0.37
Gd	5.00	20.00	11.00	13.00	23.00	1.40	5.80	14.00	4.60	4.30
Tb	0.90	4.10	2.10	2.60	4.70	0.22	1.10	2.50	0.89	0.76
Dy	5.60	28.00	14.00	18.00	32.00	1.20	6.60	16.00	5.30	5.00
Ho	1.30	6.20	2.90	3.90	7.10	0.26	1.50	3.20	1.20	1.10
Er	3.70	18.00	8.00	12.00	21.00	0.76	4.50	8.60	3.40	3.20
Tm	0.72	3.20	1.30	2.20	3.80	0.14	0.86	1.40	0.69	0.60
Yb	5.30	23.00	8.70	15.00	26.00	1.10	6.60	8.80	5.30	4.50
Lu	0.86	3.40	1.30	2.30	3.90	0.18	1.10	1.30	0.86	0.76

Table 3. Continued.

Sample	AT02-19-02A	AT02-19-04A	AT-02-19-03A	AT-02-19-05A	ATLH-02-05-07A	ATMH-02-04-01A	AT02-12-04Adup	ZE09-033B	ZE10-249
Laboratory	GSC	GSC	GSC	GSC	GSC	GSC	GSC	Actlabs(2009)	Actlabs(2011)
Latitude	59.7136	59.7126	59.7131	59.7120	59.6632	59.6488	59.7008	59.5550	59.6638
Longitude	-133.4172	-133.3990	-133.4032	-133.4009	-132.9997	-132.9074	-132.8776	-133.8780	-134.0622
Rocktype	granite	granite	granite	granite	granite	granite	granite	andesite	basalt
SiO2	73.90	72.90	76.00	71.70	73.60	73.00	73.30	61.56	52.48
Al2O3	13.80	14.30	12.40	14.30	14.20	13.80	14.00	17.17	15.27
Fe2O3(T)	0.90	1.20	1.50	2.10	1.40	2.20	1.70	6.53	8.07
MnO	0.01	0.03	0.02	0.06	0.02	0.04	0.01	0.073	0.132
MgO	0.06	0.20	0.13	0.49	0.07	0.29	0.06	2.23	6.5
CaO	0.69	0.67	0.92	1.52	0.17	1.12	0.75	3.85	8.68
Na2O	3.90	4.10	3.40	4.30	3.60	4.20	4.20	3.69	3.93
K2O	5.55	5.31	5.26	4.64	6.21	4.74	5.56	1.85	0.31
TiO2	0.12	0.17	0.15	0.34	0.11	0.25	0.11	0.648	1.351
P2O5	0.05	0.04	0.02	0.11	0.01	0.07	0.01	0.18	0.16
LOI	0.7	0.7	0.3	0.4	0.6	0.4	0.5	2.02	2.61
Total	99.8	99.8	100.3	100.1	100.2	100.2	100.2	99.8	99.48
Ba	126	299	569	785	152	338	173	2024	33
Be	7.4	7.8	5.9	8.0	5.8	7.7	7.3	<1	<1
Cr	21	23	23	34	24	24	26	50	210
Cs	13.00	5.10	6.10	5.40	14.00	7.90	16.00	0.8	0.2
Ga	30.00	20.00	24.00	20.00	31.00	22.00	32.00	18	15
Hf	11.00	5.60	8.90	6.80	10.00	8.30	11.00	3.1	2.2
Mo	2.0	7.8	15.0	9.2	0.2	0.9	0.4	<2	<2
Nb	48.00	61.00	32.00	48.00	53.00	44.00	47.00	4.6	1.8
Pb	24	23	16	16	23	20	26	10	<5
Rb	489	384	302	312	688	399	628	34	4
Sb	2.7	0.2	0.4	0.8	0.5	0.5	0.7	0.9	0.4
Sc	2.1	1.7	3.3	3.0	2.1	1.9	2.1	16	39
Sn	5.9	2.7	2.5	5.8	4.8	5.6	4.3	1	<1
Sr	11	62	61	195	11	66	-10	673	195
Ta	5.00	8.00	2.80	4.90	6.10	5.70	7.70	0.39	0.14
Th	79.00	46.00	36.00	42.00	64.00	47.00	64.00	3.81	0.22
U	35.00	19.00	10.00	17.00	25.00	18.00	16.00	2.01	0.46
Y	145.00	32.00	88.00	33.00	42.00	57.00	197.00	15.9	25.4
Zr	230.0	158.0	251.0	193.0	208.0	239.0	239.0	115	74
La	57.0	23.0	81.0	48.0	48.0	51.0	119.0	17	3.31
Ce	122.0	58.0	163.0	89.0	86.0	92.0	194.0	32.8	9.75
Pr	16.00	4.70	19.00	9.40	9.80	9.60	29.00	4	1.68
Nd	58.0	15.0	64.0	31.0	31.0	31.0	102.0	15.3	9.43
Sm	16.00	3.20	14.00	5.60	5.60	5.60	24.00	3.4	3.25
Eu	0.12	0.26	0.39	0.57	0.07	0.39	0.12	1.03	1.07
Gd	19.00	3.20	13.00	4.50	4.60	5.10	25.00	3.02	4.14
Tb	3.50	0.60	2.30	0.73	0.88	0.95	4.80	0.52	0.82
Dy	23.00	4.10	14.00	4.40	5.80	6.30	31.00	2.88	5.15
Ho	5.00	0.91	2.90	0.95	1.20	1.50	6.40	0.54	1.08
Er	14.00	2.90	7.90	2.80	3.80	4.70	19.00	1.63	3.06
Tm	2.40	0.55	1.30	0.51	0.64	0.87	2.90	0.273	0.456
Yb	16.00	4.40	8.50	3.80	4.40	6.50	20.00	1.83	2.95
Lu	2.40	0.74	1.30	0.65	0.68	1.10	2.90	0.28	0.47

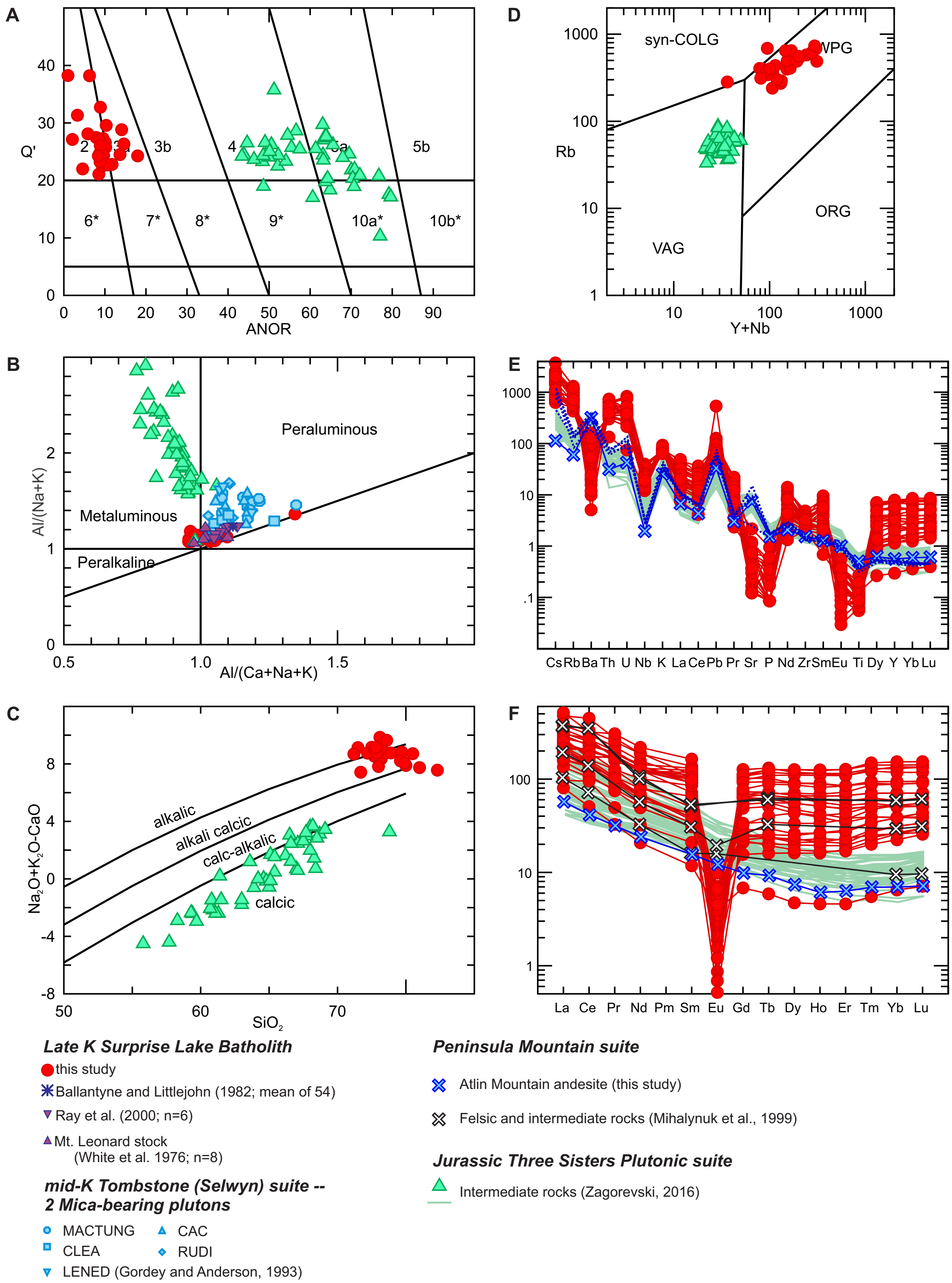

Fig. 6. Geochemical characteristics of the Surprise Lake batholith. **a)** Q'(100*Quartz/(Quartz+Orthoclase+Albite+Anorthite)) – ANOR (Anorthite/(Orthoclase+Anorthite)) plot (Whalen and Frost, 2013). **b)** Shand's index plot (Maniar and Piccoli, 1989). **c)** Modified alkali-lime index (MALI) plot (Frost et al., 2001). **d)** Tectonic discrimination plot (Pearce et al., 1984). **e)** N-MORB normalized extended trace element plot. **f)** Chondrite-normalized rare-earth element plot (normalization factors from Sun and McDonough, 1989). Tombstone plutonic suite major element data are from Anderson (1983). Surprise Lake batholith data are compiled from White et al., (1976), Ballantyne and Littlejohn (1982), Ray et al. (2000). Three Sisters Plutonic suite data are from Zagorevski (2016).

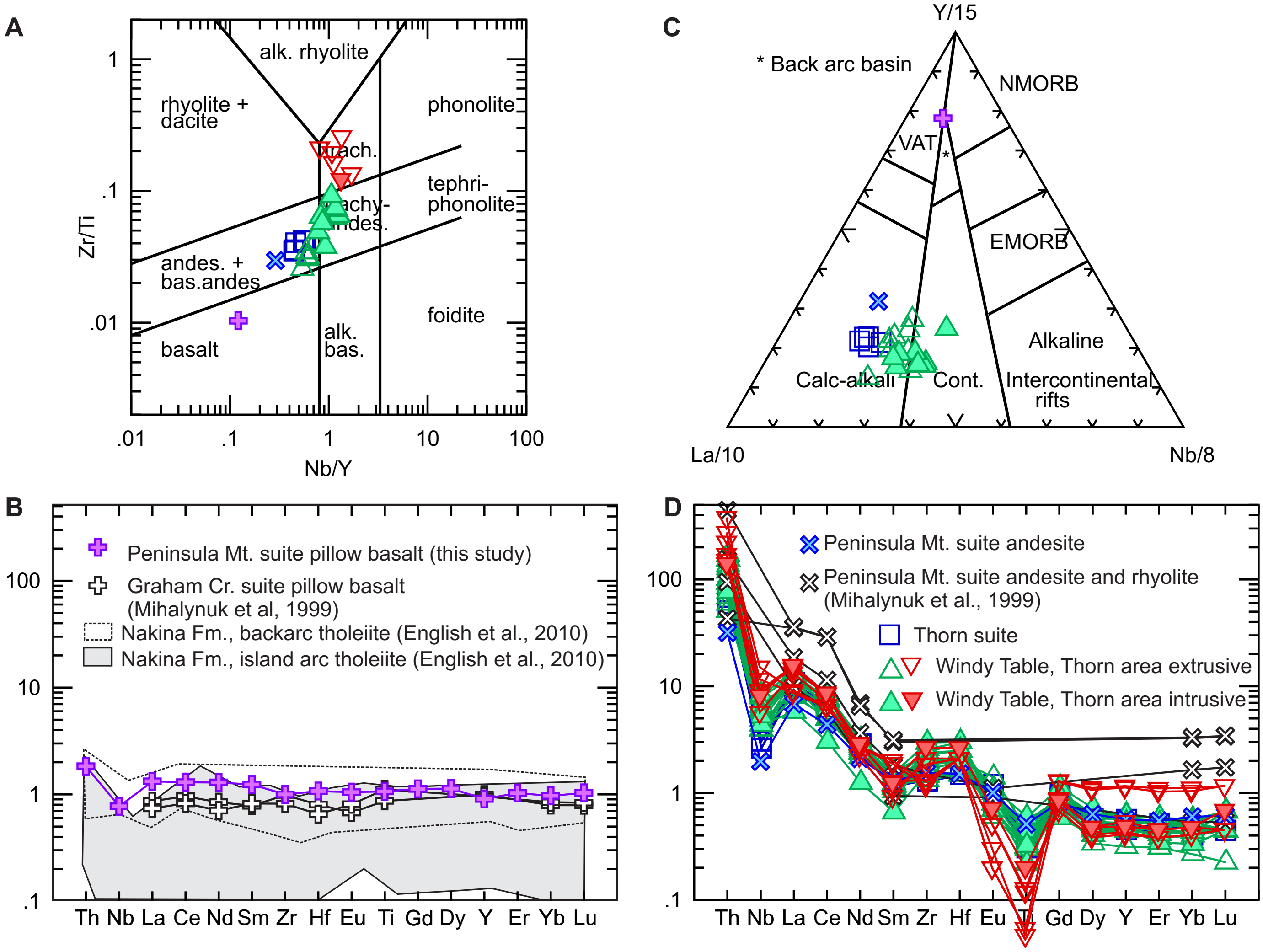

Fig. 7. Geochemical characteristics of Peninsula Mountain suite volcanic rocks. **a)** Rock type discrimination plot (Pearce, 1996). See b) and d) for symbol legend. **b)** N-MORB normalized trace element plot of Peninsula Mountain pillow basalt near headwaters of Graham Creek. **c)** Tectonic discrimination plot (Cabanis and Lecolle, 1989). **d)** N-MORB normalized (Sun and McDonough, 1989) trace element plot of Atlin Mountain andesite. Data compiled from Mihalynuk et al. (1999), Simmons et al. (2005) and English et al. (2010). N-MORB – normal mid-ocean ridge basalt, E-MORB – enriched mid-ocean ridge basalt, VAT – volcanic arc tholeiite.

5.2. Late Cretaceous magmatism, sedimentation, and tectonism

Evidence of Late Cretaceous magmatism is widespread in northwestern British Columbia and adjacent Yukon. The area to the east of Atlin Lake is mainly underlain by highly fractionated alkali-feldspar granite and monzogranite. West of Tagish Lake, Late Cretaceous magmatism is represented by relatively homogenous granodiorite. Between Tagish and Atlin lakes, Late Cretaceous volcanic and hypabyssal rocks, locally more than 1 km thick, were deposited on a high-relief angular unconformity (Bultman, 1979). East of Atlin Lake, Cretaceous supracrustal sequences are not obvious, although isolated outcrops of polymictic conglomerate containing flow-banded rhyolite clasts overlying Kedahda Formation chert may represent remnants of the basal unconformity (Fig. 4).

Existing data on Late Cretaceous volcanic rocks are sparse, but indicate an andesitic arc-like setting (Simmons et al., 2005; Fig. 7). The Surprise Lake batholith is much more evolved than the Windy-Table suite andesitic rocks and has undergone significant fractionation of plagioclase, indicated by depletion of Sr, Ba and Eu. Due to paucity of data on volcanic rocks and the highly fractionated chemistry of plutonic rocks, comparisons between the Surprise Lake batholith and coeval volcanic rocks to the west is not meaningful. Data presented herein clearly distinguish the Late Cretaceous Surprise Lake batholith from the adjacent Jurassic Fourth of July batholith and related Mount McMaster and Langrose Mountain stocks, providing a guide for regional comparisons (Fig. 6). These data highlight problems arising from tectonic discrimination of highly fractionated granites. Surprise Lake suite analyses plot in the within-plate field on the Pearce et al. (1984) diagram (Fig. 6d), yet coeval andesitic rocks suggest a calc-alkaline arc setting (Figs. 6, 7).

In the Sutlahine River area, ~150 km southeast of our study area, volcanic strata at the Thorn developed prospect may be equivalent to the Windy-Table suite. Based on U-Pb zircon age determinations, Simmons et al. (2005) identified three Late Cretaceous magmatic peaks at: ca. 93-87 Ma (Thorn suite); ca. 87 Ma (early Windy-Table suite); and ca. 82 Ma (late Windy-Table suite). The initiation of felsic magmatism in the early Windy-Table suite appears to be broadly coeval at Table Mountain (85.0 ±1.6 Ma: this study) and at Thorn (87.5 ±1.2 Ma dacite flow; SHRIMP, Simmons et al., 2005). At the Thorn developed prospect (Fig. 1), volcanic strata are as young as 81.1 ±1.5 Ma (trachyte flow, U-Pb zircon, SHRIMP; Simmons et al., 2004) and 82.8 ±0.6 Ma (rhyolite breccia U-Pb zircon, TIMS, Mihalynuk et al., 2003), overlapping the youngest felsic volcanic U-Pb zircon crystallization age at Table Mountain (81.3 ±0.3 Ma: Mihalynuk et al., 1992). The youngest Windy-Table suite felsic magmatism is coeval with the emplacement of the oldest phases of the Surprise Lake batholith (83.8 ±5 Ma: Mihalynuk et al., 1992; 81.6 ±1.1 Ma: Smith and Arehart, 2010). The youngest phases of the Surprise Lake batholith (77.5 ±1.0 Ma: Smith and Arehart, 2010) overlap the age of the biotite monzogranite near Tutshi Lake (76.5 ±1.3 Ma: this study).

The emplacement of the Windy-Table and Surprise Lake suites immediately precedes and, in part, overlaps the economically important Late Cretaceous Casino suite plutonism in Yukon (~78-72 Ma: Johnston, 1995, Selby and Creaser, 2001; Bennett et al., 2010; Allan et al., 2013; Nelson et al., 2013; Ryan et al., 2013; Mortensen et al., 2016). The Casino suite comprises volumetrically small hypabyssal rocks that yield very limited information on the processes in the underlying crust or in the now eroded volcanic carapaces. As such, more detailed investigation of the Windy-Table and Surprise Lake suites can improve the geological constraints on the late Cretaceous magmatism, including the nature and tectonic setting of the Intermontane terranes immediately before outpouring of the regionally extensive Carmacks Group basalt in Yukon (e.g., Johnston et al., 1996).

5.3. Late Cretaceous mineralization

The Surprise Lake suite and its metamorphic aureole host numerous molybdenum and granophile mineral occurrences. Mount Leonard stock hosts the Ruby Creek molybdenum deposit (also known as Adanac: 275,354,000 tonnes grading 0.067% molybdenum, measured and indicated; MINFILE 104N 052) and is possibly the source of precious metal and polymetallic base metal sulphide mineralization at the past-producing Atlin Ruffner mine. Tin and tungsten skarns adjacent to the Surprise Lake batholith (Ray et al., 2000) and cassiterite and wolframite in placer streams underlain by the batholith indicate W-Sn mineralization potential in addition to defined resources at the Ruby Creek deposit. The Surprise Lake batholith is compositionally similar to other W-Sn bearing plutonic suites, such as the Tombstone-Tungsten plutonic suite in Yukon (96-90 Ma, Anderson, 1983; Gordey and Anderson, 1993). Both suites are highly fractionated, peraluminous granites, with high alkali concentrations. Key geochemical differences between Surprise Lake and Tombstone-Tungsten suites is the more fractionated character of the Surprise Lake suite, indicated by higher K_2O and lower FeO_{total}, MgO and Sr. Late Cretaceous volcanic rocks of the Windy-Table suite host high sulphidation epithermal to transitional porphyry-style precious and base metal suphide-rich mineralization at the Thorn developed prospect, about 150 km southeast of the present study area. This mineralization is hosted by the Thorn suite plutons (ca. 93-87 Ma) and was emplaced contemporaneously with Windy-Table suite rocks (Simmons et al., 2005, Simmons et al., 2005). Highly evolved phases similar to the Surprise Lake batholith appear to be absent near Thorn (Fig. 7; Simmons et al., 2005).

Placer gold streams in the Atlin camp border the Surprise Lake batholith (e.g., Mihalynuk et al., 2017). Some streams contain tin and tungsten placers in addition to gold. Boulder Creek is known for its rich gold and wolframite placers and has its headwaters in the batholith, where tungsten showings are concentrated (Ray et al., 2000). A study of placer gold from Feather Creek (Fig. 2) identified cassiterite and thorite intergrown with gold nuggets. Both cassiterite and thorite occur within the highly fractionated Surprise Lake suite and associated skarns, but not with Jurassic Three Sisters plutonic suite or ultramafic rocks of the Cache Creek complex. Such observations led Sack and Mihalynuk (2003) to suggest a Surprise Lake batholith source for the Atlin placer gold in addition to altered ultramafic rocks (Ash, 1994; Ash et al., 2001). Subsequent collections of nuggets from other placer creeks failed to find gold intergrown with minerals of unambiguous origin (Mihalynuk et al., 2011), but did recover gold nuggets with attached phyllite from Otter Creek. In 2016, placer mining on Otter Creek discovered quartz-gold veins cutting calcareous black phyllite bedrock (Mihalynuk et al., 2017) proving that regardless of the ultimate gold source, ultramafic rocks are not a prerequisite for lode gold deposition. A placer showing on Graham Creek, west of Atlin, may also be genetically related to the Late Cretaceous magmatism rather than ultramafic rocks.

Affiliation of placer gold workings with evolved, mineralized Late Cretaceous intrusions is well established in the Yukon. For example, such placers are found in the Nansen Creek and Klaza River headwaters north of Mt. Nansen, where Yukon Tanana terrane basement rocks are cut by Early Cretaceous rocks of the Whitehorse suite plutons (Dawson Range batholith) and are overlain by coeval Mount Nansen suite volcanic strata (Yukon Geological Survey, 2016). Similarly, placer workings are directly underlain by the Mount Nansen porphyry complex and Klaza area gold-silver mineralization (Hart and Langdon, 1997; Wengzynowski et al., 2015) associated with stocks and feldspar porphyry dikes that have returned ca. 78.2-76.3 Ma U-Pb zircon crystallization ages (Mortensen et al., 2016). Placer-lode gold links in the Klaza area have also been made on the basis of detrital grain morphology and chemistry (Chapman et al., 2016).

6. Conclusion

New geochronologic and geochemical data require stratigraphic revisions in the Atlin-Tagish area (Fig. 4). New age determinations for the Surprise Lake batholith yield a crystallization age that falls in the middle of 78-82 Ma cluster determined by modern techniques. Surprise Lake batholith and comagmatic volcanic strata are part of a mineralized belt that extends into Yukon and ca. 150 km to the southeast into the Sutlahine River area. In Yukon, mineralizing Casino suite intrusions in the Klaza area are age equivalent to the mineralized Mount Leonard stock of the Surprise Lake batholith (81.6 ±1.1 to 77.5 ±1.0 Ma, Smith and Arehart, 2010). Re-Os ages for molybdenite mineralization in the Mount Leonard stock cluster around 70 Ma, significantly younger than most crystallization ages, but overlapping published cooling ages and youngest parts of the Casino suite. In the Sutlahine River area, the ~87-80 Ma Windy-Table suite is coeval with high sulphidation mineralization at the Thorn developed prospect.

Acknowledgments

Discovery Helicopters (Atlin) are gratefully acknowledged for providing logistical support and transportation in the field. This is a contribution to the Geomapping for Energy and Minerals 2, Cordillera project. Legacy data were obtained during the Targeted Geoscience Initiative: Atlin project (2001-2003). P. Sack and L. Aspler provided valuable comments that improved this manuscript.

References cited

Aitken, J.D., 1959. Atlin map-area, British Columbia. Geological Survey of Canada, Memoir 307, 89p.

Allan, M.M., Mortensen, J.K., Hart, C.J.R., Bailey, L.A., Sanchez, M.G., Ciolkiewicz, W., McKenzie, G.G., and Creaser, R.A., 2013. Magmatic and metallogenic framework of west-central Yukon and eastern Alaska. In: Colpron, M., Bissig, T., Rusk, B. G., and Thompson, J. F. H. (Eds.), Tectonics, Metallogeny, and Discovery: The North American Cordillera and similar accretionary settings. Society of Economic Geologists, Special Publication 17, 111-168.

Anderson, R.G., 1983. Selwyn plutonic suite and its relationship to tungsten skarn mineralization, southeastern Yukon and District of Mackenzie. Geological Survey of Canada, Paper 83-1B, 151-163.

Ash, C.H., 1994. Origin and tectonics setting of ophiolitic ultramafic and related rocks in the Atlin area, British Columbia (NTS 104N). Ministry of Energy, Mines and Petroleum Resources, British Columbia Geological Survey, Bulletin 94, 54p.

Ash, C.H., MacDonald, R.W., and Reynolds, P.R., 2001. Relationship between ophiolites and gold-quartz veins in the North American Cordillera. British Columbia, Ministry of Energy and Mines. British Columbia Geological Survey. Bulletin 108, 140p.

Ballantyne, S.B., and Littlejohn, A.L., 1982. Uranium mineralization and lithogeochemistry of the Surprise Lake batholith, Atlin, British Columbia. Geological Survey of Canada, Paper 81-23, 145-155.

Bennett, V., Schulze, C., Ouellette, D., and Pollries, B., 2010. Deconstructing complex Au-Ag-Cu mineralization, Sonora Gulch project, Dawson Range: A Late Cretaceous evolution to the epithermal environment. In: MacFarlane, K.E., Weston, L.H., and Blackburn, L.R. (Eds.),Yukon Exploration and Geology 2009, Yukon Geological Survey, pp. 23-45.

Bickerton, L., Colpron, M., and Gibson, D., 2013. Cache Creek terrane, Stikinia, and overlap assemblages of eastern Whitehorse (NTS 105D) and western Teslin (NTS 105C) map areas. In: MacFarlane K.E., Nordling, M.G., and Sack P.J. (Eds.), Yukon Exploration and Geology 2012, Yukon Geological Survey, pp. 1-17.

Black, L.P., Kamo, S.L., Allen, C.M., Davis, D.W., Aleinikoff, J.N., Valley, J.W., Mundil, R., Campbell, I.H., Korsch, R.J., Williams, I.S., and Foudoulis, C., 2005. Improved 206 Pb/238 U microprobe geochronology by the monitoring of a trace-element-related matrix effect; SHRIMP, ID-TIMS, ELA-ICP-MS and oxygen isotope documentation for a series of zircon standards. Chemical Geology, 205, 115-140.

Bloodgood, M.A., and Bellefontaine, K.A., 1990. The geology of the Atlin area (Dixie Lake and Teresa Island) (104N/6 and parts of 104N/5 and 12). In: Geological Fieldwork, Ministry of Energy, Mines and Petroleum Resources, British Columbia Geological Survey, Paper 1990-1, pp. 205-215.

Bloodgood, M.A., Rees, C.J., and Lefebure, D.V., 1989. Geology of the Atlin area; NTS 104N/11W, 12E. Ministry of Energy, Mines and Petroleum Resources, British Columbia Geological Survey Open File 1989-15.

Breitsprecher, K., and Mortensen, J.K., 2004. BCAge 2004A - a database of isotopic age determinations for rock units from British Columbia. British Columbia Ministry of Energy and Mines, British Columbia Geological Survey Open File 2004-3 (Release 2.0)

Bultman, T.R., 1979. Geology and tectonic history of the Whitehorse Trough west of Atlin, British Columbia. Ph.D. thesis, Yale University, 296p.

Cabanis, B., and Lecolle, M., 1989. Le diagramme La/10-Y/15-Nb/8; un outil pour la discrimination des series volcaniques et la mise en evidence des processus de melange et/ou de contamination crustale. Comptes Rendus de l'Academie des Sciences, Serie 2, Mecanique, Physique, Chimie, Sciences de l'Univers, Sciences de la Terre, 309, 2023-2029.

Chapman, R., Cook, M., Grimshaw, M., and Myles, S., 2016. Placer-lode gold relationships in the Nansen placer district, Yukon. In: MacFarlane, K.E., and Nordling, M.G (Eds.), Yukon Exploration and Geology, Yukon Geological Survey, pp. 63-78.

Christopher, P.A., and Pinsent, R.H., 1982. Geology of the Ruby Creek and Boulder Creek area near Atlin (104N/11W). Ministry of Energy, Mines and Petroleum Resources, British Columbia Geological Survey, Preliminary Map 52, 10p.

Colpron, M., and Nelson, J.L., 2011. A Digital Atlas of Terranes for the Northern Cordillera. Ministry of Energy and Mines, British Columbia Geological Survey GeoFile 2011-11.

Colpron, M., Israel, S., Murphy, D., Pigage, L., and Moynihan, D., 2016. Yukon bedrock geology map. Yukon Geological Survey Open File 2016-1, scale 1:1,000,000.

DeCelles, P.G., Ducea, M.N., Kapp, P., and Zandt, G., 2009. Cyclicity in Cordilleran orogenic systems. Nature Geoscience, 2, 251-257.

English, J.M., Mihalynuk, M.G., and Johnston, S.T., 2010. Geochemistry of the northern Cache Creek Terrane and implications for accretionary processes in the Canadian Cordillera. Canadian Journal of Earth Sciences, 47, 13-34.

Frost, B.R., Barnes, C.G., Collins, W.J., Arculus, R.J., Ellis, D.J., and Frost, C.D., 2001. A geochemical classification for granitic rocks. Journal of Petrology, 42, 2033-2048.

Gabrielse, H., Murphy, D.C., and Mortensen, J.K., 2006. Cretaceous and Cenozoic dextral orogen-parallel displacements, magmatism, and paleogeography, north-central Canadian Cordillera. In: Haggart, J.W., Enkin, R.J., and Monger, J.W.H. (Eds.), Paleogeography of the Northern American Cordillera: Evidence for and against large-scale displacements. Geological Association of Canada, Special Paper 46, 255-276.

Golding, M.L., Orchard, M.J., and Zagorevski, A., 2016. Microfossils from the Cache Creek Complex in northern British Columbia and southern Yukon. Geological Survey of Canada,

Open File 8033, 25p.
Gordey, S.P., and Anderson, R.G., 1993. Evolution of the northern Cordilleran miogeocline, Nahanni map area [105I], Yukon and Northwest Territories. Geological Survey of Canada, Memoir 428, 214p.
Gordey, S.P., McNicoll, V.J., and Mortensen, J.K., 1998. New U-Pb ages from the Teslin area, southern Yukon, and their bearing on terrane evolution in the northern Cordillera. In: Radiogenic age and isotopic studies, Geological Survey of Canada, Report 11, 129-148.
Gwillim, J.C., 1901. Atlin mining district; Geological Survey of Canada, Annual Report 1899, Volume 12, pp. B5-B48.
Hart, C.J.R., 1996. Magmatic and tectonic evolution of the Intermontane Superterrane and Coast Plutonic Complex in southern Yukon Territory. M.Sc. thesis, University of British Columbia.
Hart, C.J.R., 1997. A transect across Northern Stikinia: Geology of the Northern Whitehorse map area, Southern Yukon Territory (105D/13-16). Exploration and Geological Services Division, Yukon region, Bulletin 8, 113p.
Hart, C.J.R., and Pelletier, K.S., 1989. Geology of Carcross (105D/2) and part of Robinson (105D/7) Map Areas. Indian and Northern Affairs Canada, Open File 1989-1, 84p.
Hart, C.J.R., Goldfarb, R.J., Lewis, L.L., and Mair, J.L., 2004. The Northern Cordilleran mid-Cretaceous plutonic province: ilmenite/magnetite-series granitoids and intrusion-related mineralisation. Resource Geology, 54, 253-280.
Hart, C.J.R., and Langdon, M., 1997. Geology and mineral deposits of the Mount Nansen camp, Yukon. In: Roots, C.F. (Ed.), Yukon Exploration and Geology 1997, Exploration and Geological Services Division, Yukon, Indian and Northern Affairs Canada, 129-138.
Johnston, S.T., 1995. Geological compilation with interpretation from geophysical surveys of the northern Dawson Range, central Yukon (115-J/9 and 115-J/10, 115-J/12, 1: 100 000 scale map). Exploration and Geological Services Division, Yukon, Indian and Northern Affairs Canada, Open File 2.
Johnston, S.T., Wynne, P.J., Francis, D., Hart, C.J.R., Enkin, R.J., and Engebretson, D.C., 1996. Yellowstone in Yukon; the Late Cretaceous Carmacks Group. Geology, 24, 997-1000.
Johnston, S.T., Enkin, R.J., Baker, J., Francis, D., Colpron, M., and Larson, K., 2001. Solitary Mountain, Yukon, in Cook, F. and Erdmer, P., (Eds.), Preliminary paleomagnetic results strengthen the correlation with the Carmacks Formation. Lithoprobe SNORCLE – Cordilleran Tectonics Workshop, Victoria, Canada. 79, p. 85.
Krogh, T.E., 1982. Improved accuracy of U-Pb zircon ages by the creation of more concordant systems using an air abrasion technique. Geochimica et Cosmochimica Acta, 46, 637-649.
Lefebure, D.V., and Gunning, M.H., 1988. Yellowjacket. In: Exploration in British Columbia; 1987, Exploration in British Columbia 1987, B87-B95.
Lowe, C., Mihalynuk, M.G., Anderson, R.G., Canil, D., Cordey, F., English, J.M., Harder, M., Johnson, S.T., Orchard, M., Russell, K., Sano, H., and Villeneuve, M.E., 2003. Overview of the Atlin Integrated Geoscience Project, northwestern British Columbia, year three. Current Research - Geological Survey of Canada, 7p.
Ludwig, K.R., 2003. User's manual for Isoplot/Ex rev. 3.00. a Geochronological Toolkit for Microsoft Excel, Berkeley Geochronology Center, Berkeley, Special Publication 4, 70p.
Maniar, P.D., and Piccoli, P.M., 1989. Tectonic discrimination of granitoids. Geological Society of America Bulletin, 101, 635-643.
Massey, N.W.D., MacIntyre, D.G., Desjardins, P.J., and Cooney, R.T., 2005. Digital Map of British Columbia: Whole Province, B.C. Ministry of Energy and Mines, GeoFile 2005-1.
Mihalynuk, M.G., Johnston, S.T., English, J.M., Cordey, F., Villeneuve, M.E., Rui, L., and Orchard, M.J., 2003a. Atlin TGI; Part II, Regional geology and mineralization of the Nakina area (NTS 104N/2W and 3). In: Geological Fieldwork 2002, British Columbia Ministry of Energy and Mines, British Columbia Geological Survey, pp. 9-37.
Mihalynuk, M.G., Devine, F.A.M., and Friedman, R.M., 2003b. Marksmen partnership - potential for shallow submarine VMS (Eskay-style) and intrusive-related gold mineralization, Tutshi Lake Area. British Columbia Ministry of Energy and Mines, British Columbia Geological Survey, Geofile 2003-9.
Mihalynuk, M.G., Mountjoy, K.J., Smith, M.T., Currie, L.D., Gabites, J.E., Tipper, H.W., Orchard, M.J., Poulton, T.P., and Cordey, F., 1999. Geology and mineral resources of the Tagish Lake area (NTS 104M/8,9,10E, 15 and 104N/12W), northwestern British Columbia. British Columbia Ministry of Energy and Mines, Energy and Minerals Division, Geological Survey Branch, Bulletin 105, 202p.
Mihalynuk, M.G., Smith, M.T., Gabites, J.E., Runkle, D., and Lefebure, D., 1992. Age of emplacement and basement character of the Cache Creek Terrane as constrained by new isotopic and geochemical data. Canadian Journal of Earth Sciences, 29, 2463-2477.
Mihalynuk, M.G., Smyth, W.R., Mountjoy, K.J., McMillan, W.J., Ash, C.H., and Hammack, J.L., 1991. Highlights of 1990 fieldwork in the Atlin area. In: Geological Fieldwork, 1990 Ministry of Energy, Mines and Petroleum Resources, British Columbia Geological Survey Paper 1991-1, pp. 145-152.
Mihalynuk, M.G., Ambrose, T.K., Devine, F.A.M., and Johnston, S.T., 2011. Atlin placer gold nuggets containing mineral and rock matter: implications for lode gold exploration. In: Geological Fieldwork 2010, British Columbia Ministry of Energy and Mines, British Columbia Geological Survey Paper 2010-1, pp. 65-72.
Mihalynuk, M.G., Zagorevski, A., Orchard, M.J., English, J.M., Bidgood, A.K., Joyce, N., and Friedman, R.M., 2017. Geology of the Sinwa Creek area (104K/14). In: Geological Fieldwork 2016, British Columbia Ministry of Energy and Mines, British Columbia Geological Survey Paper 2017-1, this volume.
Milidragovic, D., Joyce, N.L., Zagorevski, A., and Chapman, J.B., 2016. Petrology of explosive Middle-Upper Triassic ultramafic rocks in the Mess Creek area, northern Stikine terrane. In: Geological Fieldwork 2015, British Columbia Ministry of Energy and Mines, British Columbia Geological Survey Paper 2016-1, pp. 95-111.
Monger, J.W.H., 1975. Upper Paleozoic rocks of the Atlin Terrane, northwestern British Columbia and south-central Yukon. Paper 74-47, Geological Survey of Canada, 73p.
Monger, J.W.H., 1977. Upper Paleozoic rocks of northwestern British Columbia. Geological Survey of Canada, Paper 77-1A, 255-262.
Mortensen, J.K., Hart, C.J.R., Tarswell, J., and Allan, M.M., 2016. U-Pb zircon age and Pb isotopic constraints on the age and origin of porphyry and epithermal vein mineralization in the eastern Dawson Range, Yukon. In: Yukon Exploration Geology 2015, MacFarlane, K.E., and Nordling, M.G., (Eds.), Yukon Geological Survey, pp. 165-185, including appendices.
Nelson, J.L., Colpron, M., and Israel, S., 2013. The Cordillera of British Columbia, Yukon, and Alaska: tectonics and metallogeny. In: Colpron, M., Bissig, T., Rusk, B.G., and Thompson, J.F.H., (Eds.), Tectonics, Metallogeny, and Discovery: The North American Cordillera and similar accretionary settings, Society of Economic Geologists, Special Publication 17, 53-109.
Parrish, R.R., Roddick, J.C., Loveridge, W.D., and Sullivan, R.W., 1987. Uranium-lead analytical techniques at the Geochronology Laboratory, Geological Survey of Canada. Geological Survey of Canada, Paper 87-2, 3-7.
Pearce, J.A., 1996. A user's guide to basalt discrimination diagrams. In: Wyman, D. A., (Ed.), Trace element geochemistry of volcanic rocks: Applications for massive sulphide exploration, Geological

Association of Canada, Short Course, Volume 12, 79-113.
Pearce, J.A., Harris, N.B.W., and Tindle, A.G., 1984. Trace element discrimination diagrams for the tectonic interpretation of granitic rocks. Journal of Petrology, 25, 956-983.
Ray, G.E., Meinert, L.D., Webster, I.C.L., Ballantyne, S.B., Kilby, C.E., Cornelius, S.B., Lentz, D.R., and Newberry, R.J., 2000. The geochemistry of three tin-bearing skarns and their related plutonic rocks, Atlin, northern British Columbia. Economic Geology, 95, 1349-1365.
Roddick, J.C., Loveridge, W.D., and Parrish, R.R., 1987. Precise U/Pb dating of zircon at the sub-nanogram Pb level. Chemical Geology, Isotope Geoscience Section, 66, 111-121.
Ryan, J.J., Zagorevski, A., Williams, S.P., Roots, C., Ciolkiewicz, W., Hayward, N., and Chapman, J.B., 2013. Geology, Stevenson Ridge (northeast part), Yukon: Geological Survey of Canada, Canadian Geoscience Map 116.
Sack, P.J., and Mihalynuk, M.G., 2003. Proximal gold-cassiterite nuggets and composition of the Feather Creek placer gravels: clues to a lode source near Atlin, B.C. In: Geological Fieldwork 2003, British Columbia Ministry of Energy and Mines, British Columbia Geological Survey Paper 2003-1, pp. 147-161.
Selby, D., and Creaser, R.A., 2001. Late and Mid-Cretaceous mineralization in the northern Canadian Cordillera; constraints from Re-Os molybdenite dates. Economic Geology, 96, 1461-1467.
Simmons, A.T., Tosdal, R.M., Baker, D., Friedman, R., and Ullrich, T.D., 2005. Late Cretaceous volcanoplutonic arcs in northwestern British Columbia: implications for porphyry and epithermal deposits. In: Geological Fieldwork 2004, British Columbia Ministry of Energy, Mines and Petroleum Resources, British Columbia Geological Survey Paper 2005-1, pp. 347-360.
Smith, J.L., and Arehart, G.B., 2010. Isotopic investigation of the Adanac porphyry molybdenum deposit in northwestern British Columbia (NTS 104N/11); final project report. Geoscience BC Report, 2010-1, 115-126.
Stacey, J.S., and Kramers, J.D., 1975. Approximation of terrestrial lead isotope evolution by a two-stage model. Earth and Planetary Science Letters, 26, 207-221.
Stern, R.A., 1997. The GSC Sensitive High Resolution Ion Microprobe (SHRIMP); analytical techniques of zircon U-Th-Pb age determinations and performance evaluation. In: Current Research, Geological Survey of Canada Paper 1997-F, 1-3.1.
Stern, R.A., and Amelin, Y., 2003. Assessment of errors in SIMS zircon U-Pb geochronology using a natural zircon standard and NIST SRM 610 glass. Chemical Geology, 197, 111-142.
Sun, S.S., and McDonough, W.F., 1989. Chemical and isotopic systematics of oceanic basalts; implications for mantle composition and processes. Geological Society Special Publication, 42, 313-345.
Watson, K.D., and Mathews, W.H., 1944. The Tuya-Teslin area, northern British Columbia. British Columbia Department of Mines. British Columbia Geological Survey Bulletin 19, 52p.
Wengzynowski, W.A., Giroux, G.H., and Martin, C.J., 2015. NI43-101 technical report describing geology, mineralization, geochemical surveys, geophysical surveys, diamond and percussion drilling, metallurgical testing and mineral resources on the Klaza property Yukon, Canada. SEDAR filing, and https://www.rockhavenresources.com/assets/projects/2015-06-19_Klaza_NI-43-101.pdf [accessed November, 2016].
Whalen, J., and Frost, C., 2013. The Q-ANOR diagram: A tool for the petrogenetic and tectonomagmatic characterization of granitic suites. Geological Society of America Abstracts with Programs, 45, 24.
White, W.H., Stewart, D.R., and Ganster, M.W., 1976. Adanac (Ruby Creek). Canadian Institute of Mining and Metallurgy, Special Volume 15, pp. 476-483.
Zagorevski, A., 2016. Geochemical data of the northern Cache Creek and Stikine terranes and their overlap assemblages, British Columbia and Yukon; Geological Survey of Canada, Open File 8039, 1 .zip file.